Earth and Planetary Science Letters 272 (2008) 158–171

Contents lists available at ScienceDirect

Earth and Planetary Science Letters

journal homepage: www.elsevier.com/locate/epsl

Eocene melting of subducting continental crust and early uplifting of central Tibet: Evidence from central-western Qiangtang high-K calc-alkaline andesites, dacites and rhyolites

Qiang Wang [a,b,c,*], Derek A. Wyman [b,*], Jifeng Xu [a], Yanhui Dong [a], Paulo M. Vasconcelos [d], N. Pearson [e], Yusheng Wan [c], Han Dong [f], Chaofeng Li [g], Yuanshan Yu [f], Tongxing Zhu [f], Xintao Feng [f], Qiyue Zhang [f], Feng Zi [a], Zhuyin Chu [g]

[a] Key Laboratory of Isotope Geochronology and Geochemistry, Guangzhou Institute of Geochemistry, Chinese Academy of Sciences, Guangzhou 510640, PR China
[b] School of Geosciences, Division of Geology and Geophysics, The University of Sydney, NSW 2006, Australia
[c] Chinese Academy of Geological Science, 26 Beiwanzhuang Road, Beijing 100037, PR China
[d] Department of Earth Sciences, University of Queensland, Brisbane, Qld 4072, Australia
[e] ARC National Key Centre for Geochemical Evolution and Metallogeny of Continents (GEMOC), Department of Earth and Planetary Sciences, Macquarie University, Sydney, NSW 2109, Australia
[f] Chengdu Institute of Geology and Mineral Resources, Chengdu 610082, PR China
[g] Institute of Geology and Geophysics, Chinese Academy of Sciences, Beijing, 100029, PR China

ARTICLE INFO

Article history:
Received 4 July 2007
Received in revised form 15 April 2008
Accepted 23 April 2008
Available online 9 May 2008

Editor: C.P. Jaupart

Keywords:
adakites
high-Mg andesites
peraluminous
subduction
uplift
Eocene
Qiangtang
Tibet

ABSTRACT

Changes in oceanic O–Sr isotopic compositions and global cooling beginning in the Eocene are considered to have been caused by the uplift of the Tibetan Plateau. The specific timing and uplift mechanism, however, have long been subjects of debate. We investigated the Duogecuoren lavas of the central-western Qiangtang Block, which form the largest outcrops among Cenozoic lavas in northern-central Tibet and have widely been considered as shoshonitic. Our study demonstrates, however, that most of these lavas are high-K calc-alkaline andesites, dacites and rhyolites. Moreover, they are characterized by high Sr (367–2472 ppm) and Al_2O_3 (14.55–16.86 wt.%) and low Y (3.05–16.9 ppm) and Yb (0.31–1.48 ppm) contents and high La/Yb (27–100) and Sr/Y (48–240) ratios, similar to adakitic rocks derived by partial melting of an eclogitic source. They can be further classified as either peraluminous and metaluminous subtypes. The peraluminous rocks have relatively high SiO_2 (>66 wt.%) contents, and low MgO (<1.0 wt.%), Cr (4.94–23.3 ppm) and Ni (2.33–17.0 ppm) contents and $Mg^{\#}$ (20–50) values, while the metaluminous rocks exhibit relatively low SiO_2 (55–69 wt.%) contents, and high MgO (1.41–6.34), Cr (25.7–383 ppm), Ni (14.13–183 ppm) and $Mg^{\#}$ (46–69) values, similar to magnesian andesites. $^{40}Ar/^{39}Ar$ and SHRIMP zircon U–Pb dating reveal that both peraluminous and metaluminous adakitic rocks erupted in the Eocene (46–38 Ma). Paleocene–Early Miocene thrust faults and associated syn-contractional basin deposits in the Qiangtang Block suggest that this region was undergoing crustal shortening within a continent during the Eocene. The low ε_{Nd} (−2.81 to −6.91) and high $^{87}Sr/^{86}Sr$ (0.7057–0.7097), Th (11.2–32.3 ppm) and Th/La (0.23–0.88) values in the Duogecuoren adakitic rocks further indicate that they were not derived by partial melting of subducted oceanic crust. Taking into account tectonic and geophysical data and the compositions of xenoliths in Cenozoic lava in northern-central Tibet, we suggest that the peraluminous adakitic rocks were most probably derived by partial melting of subducted sediment-dominated continent of the Songpan-Ganzi Block along the Jinsha suture to the north at a relatively shallow position (the hornblende+garnet stability field), but the metaluminous adakitic rocks likely originated from the interaction between peraluminous adakitic melts generated at greater depths (the garnet+rutile stability field) and mantle. Because the Duogecuoren adakitic rocks must have originated from a garnet-bearing (namely, eclogite facies) source, Eocene continental subduction along the Jinsha suture caused the thickening of the Qiangtang crust. Given that crustal thickening generally equates with elevation, the uplift of the Central Tibetan Plateau probably began as early as 45–38 Ma, which provides important evidence for tectonically driven models of oceanic O–Sr isotope evolution during global cooling and Asian continental aridification beginning in the Eocene.

* Corresponding authors. Wang is to be contacted at Key Laboratory of Isotope Geochronology and Geochemistry, Guangzhou Institute of Geochemistry, Chinese Academy of Sciences, Guangzhou 510640, PR China.
E-mail addresses: wqiang@gig.ac.cn (Q. Wang), dwyman@geosci.usyd.edu.au (D.A. Wyman).

0012-821X/$ – see front matter © 2008 Elsevier B.V. All rights reserved.
doi:10.1016/j.epsl.2008.04.034

1. Introduction

Changes in oceanic O–Sr isotopic composition, global cooling and Asian continental aridification beginning in the Eocene have been attributed to the uplift of the Tibetan Plateau (Dupont-Nivet et al., 2007; Raymo and Ruddiman, 1992; Ruddiman, 1998). However, the time and mechanism of uplift remain unclear. A widely accepted interpretation is that the rapid uplift of west (i.e., west of about 92°E) and southeast (i.e., east Qiangtang) Tibetan Plateau began around 20–13 Ma (e.g., Blisniuk et al., 2001; Harris, 2006; Molnar et al., 1993; Turner et al., 1996) and 40–30 Ma (Chung et al., 1998) ago, respectively, in response to the convective removal of the lower portion of the thickened Asian lithosphere (e.g., Molnar et al., 1993). Recently, an alternative interpretation argues that uplift of the Tibetan Plateau was stepwise, and initiated from the central block (i.e., Qiangtang) in the Eocene and then northwards and southwards after the Eocene, in response to the subduction of Asian or Indian continental lithosphere (e.g., Roger et al., 2000; Tapponnier et al., 2001). Despite the differing mechanisms, both hypotheses emphasize that uplift of the southeast Tibet Plateau (i.e., east Qiangtang) was initiated in the Eocene, based mainly on occurrences of 51–30 Ma shoshonitic (or potassic) and minor calc-alkaline magmatic rocks (e.g., Chung et al., 1998; Roger et al., 2000; Spurlin et al., 2005; Tapponnier et al., 2001). In contrast, Kohn and Parkinson (2002) argued that the eruption of Eocene shoshonitic lavas in the east Qiangtang Block has no implications for topography of the Tibetan Plateau, and Chung et al. (2005) suggest that Eocene shoshonitic lavas in the east Qiangtang Block were actually related to back-arc extension rather than the convective removal of the lower portion of the thickened Asian lithosphere. Accordingly, they argue against any Eocene uplift in the east Qiangtang Block. In the west Qiangtang Block (i.e., west of about 92°E), most Cenozoic volcanic rocks have been considered to be shoshonitic and were generated only during the past 15–3 Ma (e.g., Chung et al., 1998, 2005; Turner et al., 1996; Williams et al., 2004), similar to some late (16–0 Ma) shoshonitic rocks in the east Qiangtang Block (Wang et al., 2001). Minor exceptions are sporadic outcrops of 31–29 Ma shoshonitic rocks in the Yulinshan area and 45 Ma Na-rich basalts in the Bangdaco area (Ding et al., 2003).

Given that the question of whether Eocene uplift of the Tibetan Plateau took place is so important for interpreting global climate change and shifts in oceanic isotope composition, our study has focused on two fundamental problems regarding Cenozoic lavas in the Qiangtang Block: (1) Did large-scale lavas erupt in the west Qiangtang Block during the Eocene? (2) If so, did eruption of the lavas have implications for the topography of the Tibetan Plateau?

In this study, we mainly report the geochronology and geochemistry data of the Duogecuoren lavas from the west Qiangtang Block, which have the largest outcrop area among Cenozoic lavas in northern-central Tibet. Geochronological and geochemical data suggest that they are mainly Eocene (46–38 Ma) high-K calc-alkaline rocks with adakite geochemical characteristics, which may be derived by partial melting of eclogitic rocks (e.g., Atherton and Petford, 1993; Defant and Drummond, 1990; Rapp et al., 2003). Moreover, they are distinct from Miocene (18–15 Ma) low-MgO adakites in Northern Tibet (Wang et al., 2005), and include both peraluminous-low-MgO and metaluminous-high-MgO adakitic subtypes. Their distinctive

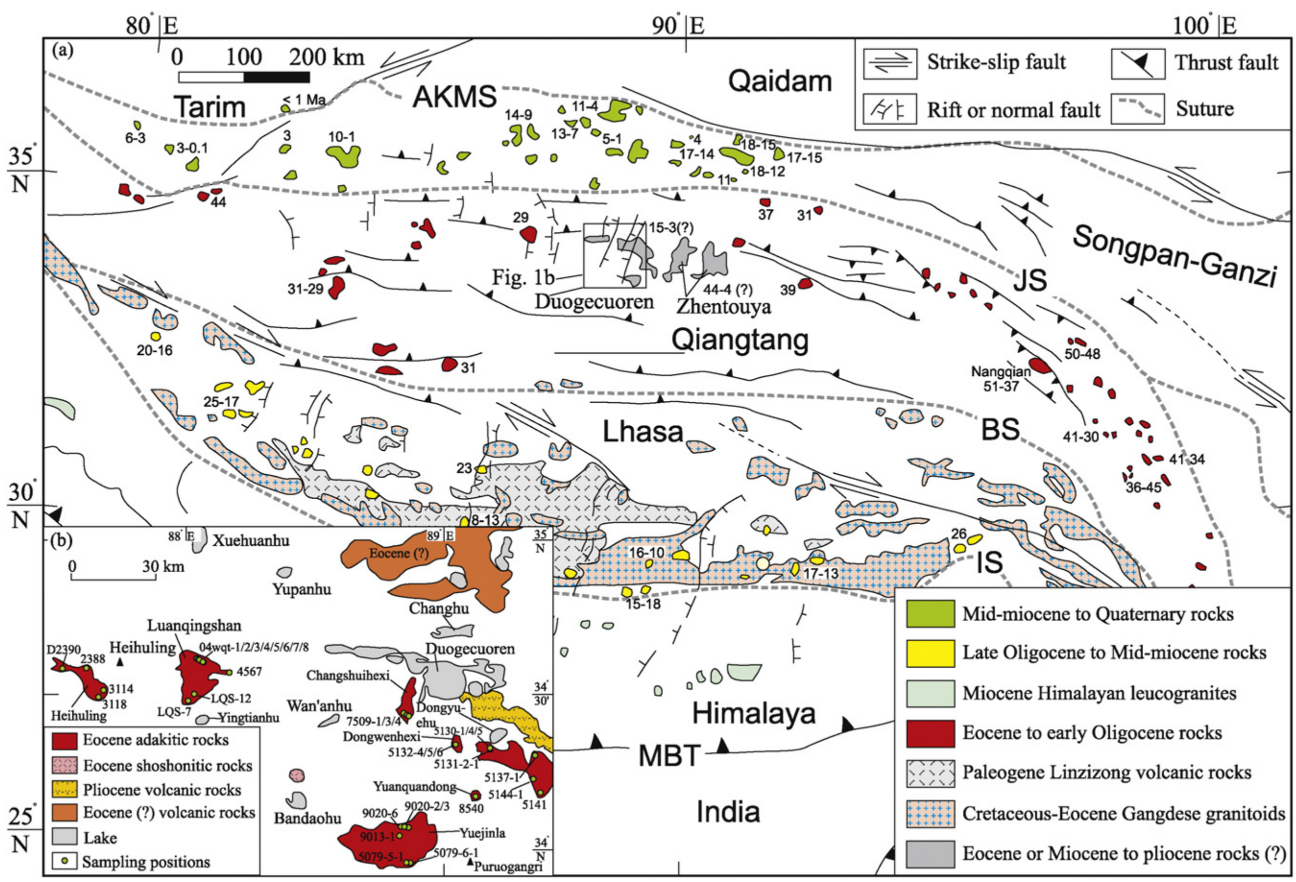

Fig. 1. (a) Map of Tibetan Plateau showing major blocks and temporal–spatial distribution of Cenozoic volcanic rocks (modified from diagrams of Yin and Harrison, 2000; Chung et al., 2005). Ages shown for volcanic rocks are from Ding et al. (2003), Chung et al. (2005), Wang et al. (2005), Guo et al. (2006), and references therein, and from this study. Main suture zones between major blocks: AKMS—Anyimaqen–Kunlun–Muztagh; JS—Jinshajiang; BS—Bangong; IS—Indus. Major faults: MBT—Main Boundary thrust. (b) Simplified geologic map showing outcrops of magmatic rocks in Duogecuoren area, west Qiangtang, northern Tibet.

petrogenesis provides an important constraint on the time and mechanism of the uplift in Central Tibet.

2. Geological setting

On a large scale, the Tibetan Plateau constitutes a tectonic collage of continental blocks (terranes). From north to south, the interior of the Tibetan Plateau comprises the roughly east–west-trending Songpan-Ganzi, Qiangtang and Lhasa blocks (Fig. 1a) (Chung et al., 2005; Yin and Harrison, 2000). The Qiangtang Block is bounded by the Jinshajiang suture to the north, and the Bangong suture to the south (Yin and Harrison, 2000). It is generally accepted that the suturing of the Songpan-Ganzi–Qiangtang and Qiangtang–Lhasa blocks occurred in the Middle Cretaceous (Yin and Harrison, 2000), and consequently the Qiangtang Block has been in an intra-continental setting since that time.

Cenozoic magmatic rocks are unevenly distributed in the Qiangtang Block and are mainly concentrated in the northern part of the block close to the Jinshajiang suture (Fig. 1a). Previous studies indicated that, apart from minor calc-alkaline granites and rhyodacites, most are shoshonitic in composition, and their eruption ages range from ca. 51 to 0 Ma (Turner et al., 1996; Chung et al., 1998, 2005; Deng, 1998; Hacker et al., 2000; Roger et al., 2000; Yin and Harrison, 2000; Wang et al., 2001; Ding et al., 2003; Williams et al., 2004; Spurlin et al., 2005; Jiang et al., 2006; Mo et al., 2006; Guo et al., 2006; Liang et al., 2007). The lavas of the Duogecuoren–Zhentouya area in the west Qiangtang Block display the largest outcrop areas of all Cenozoic magmatic rocks in the central-northern Tibetan Plateau (Fig. 1a). Previously, the Duogecuoren lavas (Fig. 1a) had been considered to be Miocene–Pliocene (e.g., Turner et al., 1996; Chung et al., 1998, 2005; Lai et al., 2003; Williams et al., 2004). Our new field investigations suggest that Cenozoic volcanic rocks are widely distribute in the Duogecuoren area in outcrops that range from 600–700 m^2 to several km^2 in size (Fig. 1b). Our more comprehensive data set (see Appendices A–G) suggests that, except for ~3 Ma lavas in the northern Dongyuehu area (Hacker et al., 2000), all of the volcanic rocks are of Eocene age (46–38 Ma), as discussed below (Fig. 1b). Moreover, except for the shoshonitic lavas in the Bandaohu area, the Eocene lavas are adakitic (with features such as high Sr/Y ratios, high Sr concentrations, and very low Y and heavy rare earth element [REE] contents).

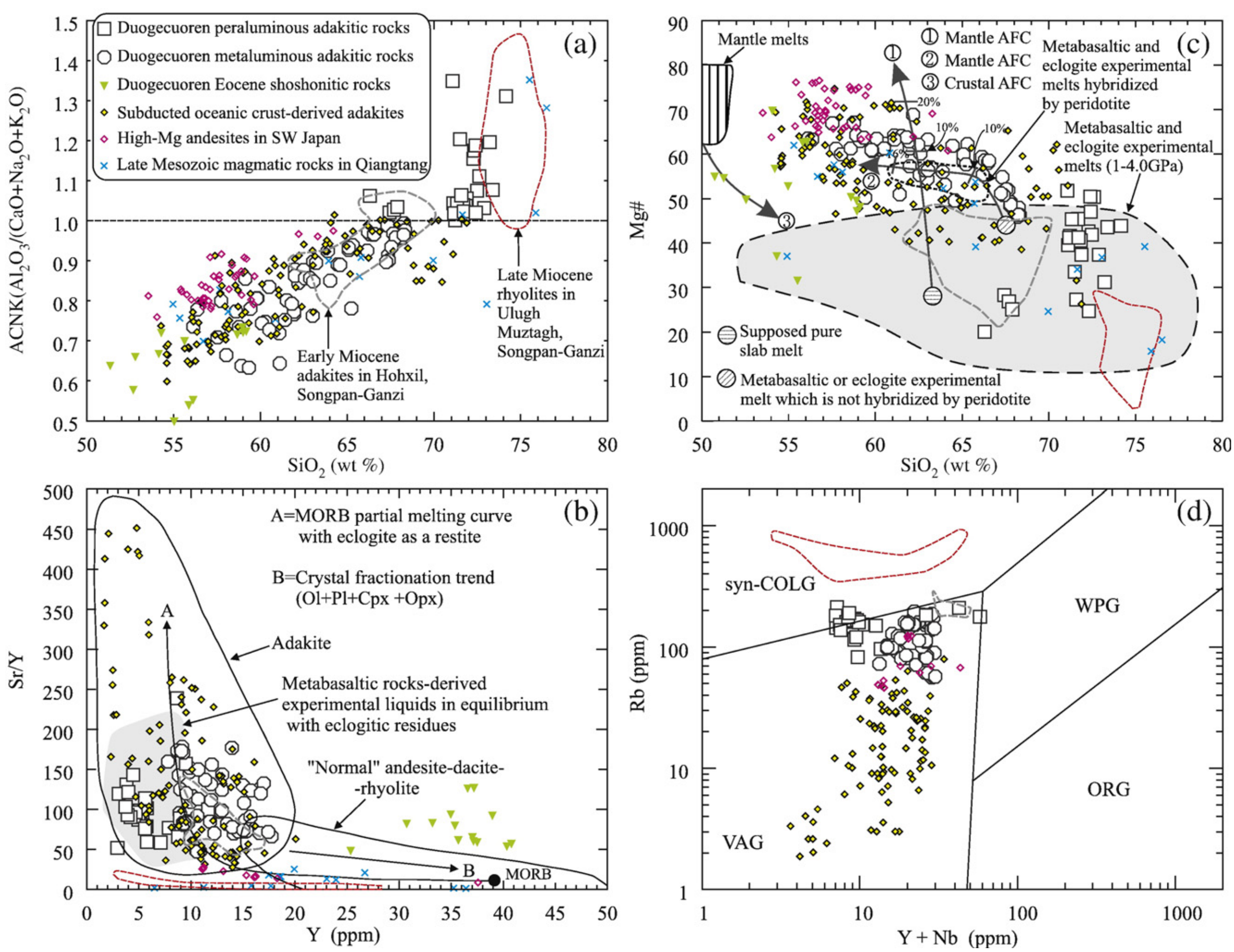

Fig. 2. (a) SiO_2 (wt.%) versus ACNK ($Al_2O_3/(CaO+Na_2O+K_2O)$) diagram. (b) Y (ppm) versus Sr/Y diagram (after Defant et al., 2002). (c) SiO_2 (wt.%) versus $Mg^{\#}$ ($100\times Mg^{2+}/(Fe^{2+}+Mg^{2+})$) diagram. Mantle AFC curves, with proportions of assimilated peridotite indicated, are after Stern and Kilian (1996) (Curve 1) and Rapp et al. (1999) (Curve 2). Crustal AFC is after Stern and Kilian (1996). The data for metabasaltic and eclogite experimental melts (1–4.0 GPa), and peridotite-hybridized equivalents, are from Rapp et al. (1999, 2003) and references therein. (d) Y+Nb (ppm) versus Rb diagram (after Pearce et al., 1984). The field for Early Miocene adakitic rocks in the Hohxil area of the Songpan-Ganzi Block is constructed using data of Wang et al. (2005). The field for Late Miocene rhyolites in the Ulugh Muztagh area of the Songpan-Ganzi Block is constructed using data of McKenna and Walker (1990). The data for High-Mg andesites in SW Japan are from Shimoda et al. (1998), Tatsumi (2001), Tatsumi and Hanyu (2003), and reference therein; Late Mesozoic magmatic rocks in Qiangtang are from Li et al. (2005) and Liao et al. (2005); the data for the subducted oceanic crust-derived adakites are from Defant et al. (2002) and Martin et al. (2005), and references therein; the data for the Duogecuoren shoshonitic rocks are from unpublished data of Q. Wang. The data for the Duogecuoren adakitic rocks are from Appendix A and unpublished data of Y. Dong.

3. Analytical methods

Two samples for SHRIMP zircon U–Pb dating were collected from the low-MgO-peraluminous adakitic rock (D2390) in the Heihuling area and high-MgO-metaluminous adakitic rock (5144-1) in the southern Dongyuehu Lake area. Zircon grains were separated using conventional heavy liquid and magnetic techniques. Zircon grains were handpicked and mounted in an epoxy resin disc, and then polished and coated with gold film. Internal morphology was examined using cathodoluminescence images prior to U–Pb isotopic analyses. The U–Pb isotopic analyses were performed using the Sensitive High-Resolution Ion Microprobe (SHRIMP-II) at the Chinese Academy of Geological Science (Beijing). Details of the analytical procedures of zircon analysis using SHRIMP have been given by Jian et al. (2003). One sample for LAM-ICP-MS zircon U–Pb dating was collected from the shoshonitic rock (8524-1) in the Bandaohu area. Zircon grains were separated using conventional heavy liquid and magnetic techniques. The separated zircons were sorted under a Leica binocular microscope fitted with UV light, and a representative set of each distinct morphological population was mounted in epoxy blocks and polished for analysis. Cathodoluminescence images were

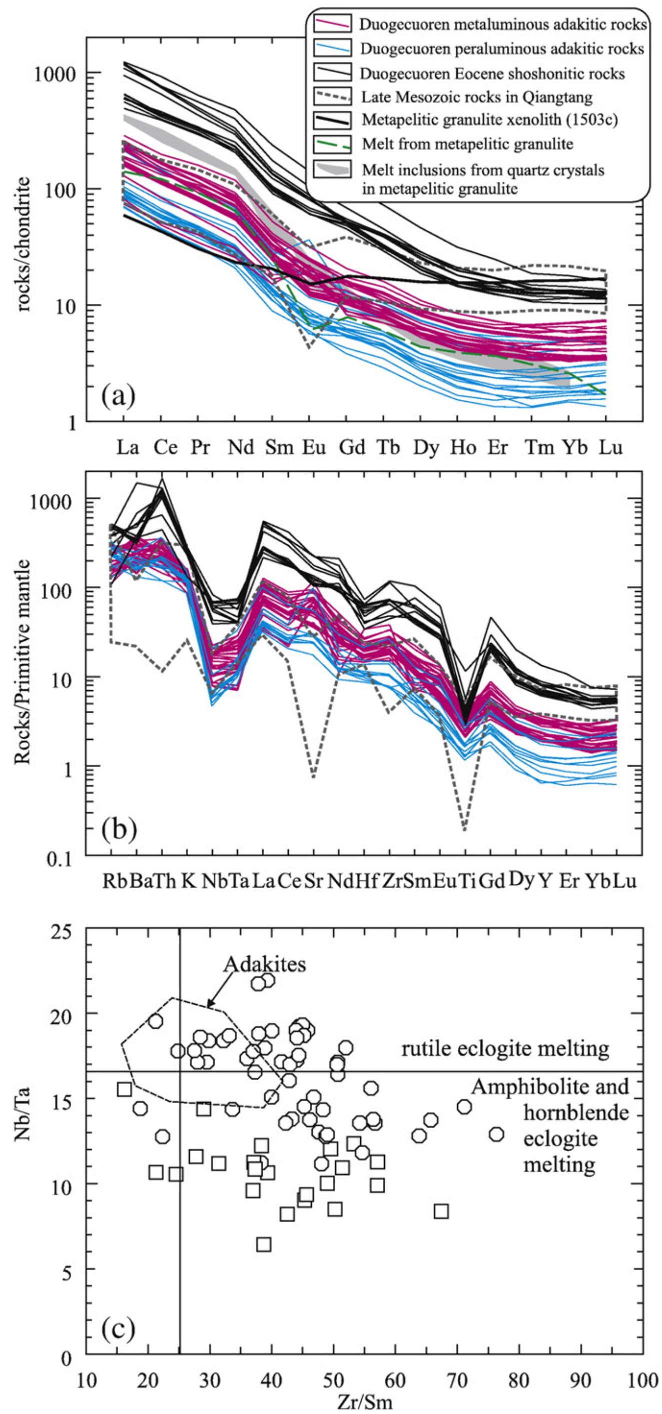

Fig. 3. (a) Chondrite-normalized rare earth element (REE) patterns for the Duogecuoren magmatic rocks. Late Mesozoic magmatic rocks in Qiangtang are from Li et al. (2005) and Liao et al. (2005). The data for metapelitic granulite xenolith (1503c) and melt inclusions from quartz crystals in metapelitic granulite are from Hacker et al. (2005). Chondrite normalizing values are from Boynton (1984). (b) Primitive mantle-normalized rare earth element (REE) patterns for the Duogecuoren magmatic rocks. Primitive mantle normalizing values are from Sun and McDonough (1989). (c) Nb/Ta versus Zr/Sm diagram (after Condie, 2005). The field of slab-derived adakites and melting fields are after Condie (2005). The data for the Duogecuoren shoshonitic rocks are from unpublished data of Q. Wang. The data for the Duogecuoren adakitic rocks are from Appendix A and unpublished data of Y. Dong.

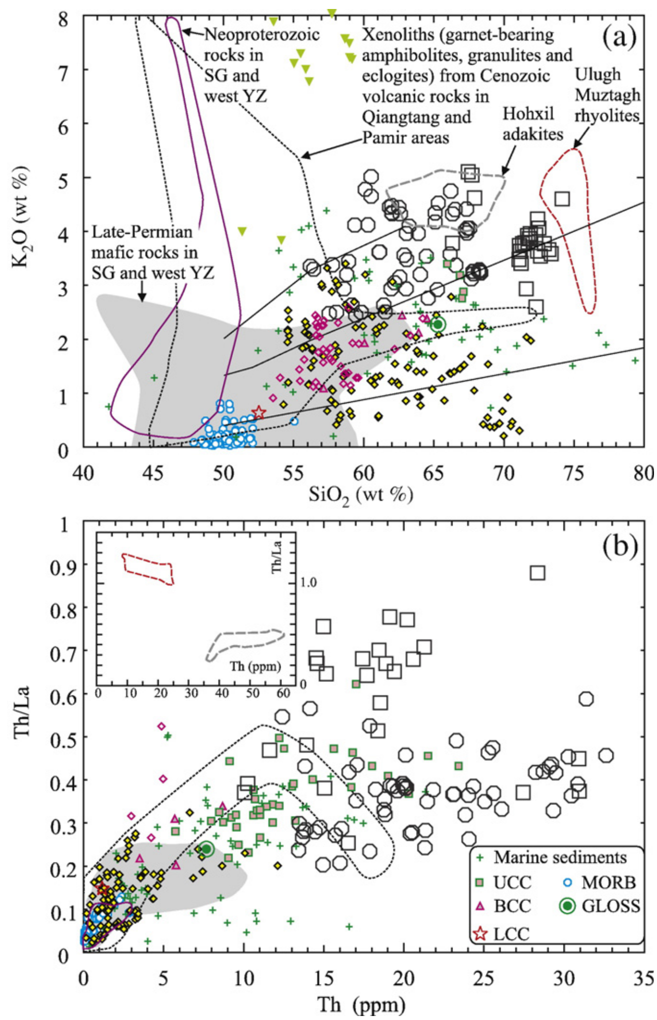

Fig. 4. (a) SiO_2 (wt.%) versus K_2O diagram. (b) Th versus Th/La diagram. The field for the xenoliths (garnet-bearing amphibolites, granulites and eclogites) from Cenozoic volcanic rocks in the Qiangtang and Pamir areas is constructed using data of Deng et al. (1998) and Hacker et al. (2005). The field for Late Permian mafic rocks in the Songpan-Ganzi (SG) and west Yangtze (YZ) Block is constructed using data of Xu et al. (2001) and Song et al. (2004). The field for the Neoproterozoic rocks in the Songpan-Ganzi and west Yangtze Blocks is constructed using data of Li et al. (2003). The data for marine sediments and GLOSS (global subducting sediment) are from Plank and Langmuir (1998). The data for BCC (bulk continental crust), LCC (lower continental crust) and UCC (upper continental crust) are from Condie (1993), Plank (2005), and references therein. MORB data are from Niu and Batiza (1997). Other data (e.g., the Hohxil adakitic rocks and Ulugh Muztagh rhyolites) are the same as in Fig. 2.

collected using a Cameca SX100 electron microprobe (EMP) at GEMOC Key Centre, Macquarie University and these were used to examine internal structure. U–Pb dating was performed at GEMOC Key Centre, using a New Wave Research LUV213 laser system attached to an Agilent 7500s inductively-coupled plasma mass spectrometer (ICP-MS). The analytical procedures for the U–Pb dating are described in detail in Jackson et al. (2004). Laser operating conditions used in this study included a spot size of 30 μm, a repetition rate of 5 Hz and a beam energy of 0.2 J cm^{-2} (measured in a beam splitter). Common Pb was corrected by ComPbCorr#3_151 (Andersen, 2002) for those with common $^{206}Pb>1\%$.

Selected relatively fresh whole rock chips were ultrasonically cleaned in distilled water with <5% HNO_3 and distilled water, successively, and then dried and handpicked to remove visible contamination. Argon isotope analyses for 6 samples were conducted on a MM-1200 mass spectrometer at the Laboratory of analyzing center, Guilin Resource and Geological Institute following procedures similar to those described in detail by Wang et al. (2007a). The rock chips were wrapped in Sn foil and sealed in 6-mm-ID evacuated quartz-glass vials together with ZBH-25 (biotite) flux monitors, and irradiated for 37 h at the Beijing Nuclear Research Center. The monitor samples were individually fused and analyzed for argon-isotope compositions. All samples were step-heated using a radio-frequency furnace. Argon isotope analyses were conducted on a MM-1200 mass spectrometer at the Laboratory of analyzing center, Guilin Resource and Geological Institute. The monitor standard was the ZBH-25 (biotite, 132.5 Ma). All errors are quoted at the 1*s* level and do not include the uncertainly of the monitor age. Argon isotope analyses for the other 3 samples were conducted at the UQAGES (University of Queensland Argon Geochronology in Earth Sciences) laboratory following procedures detailed by Vasconcelos (1999). Ten to 20 pure grains from each sample were loaded into irradiation disks along with Fish Canyon standards (28.02 Ma) (Renne et al., 1998). The disks were wrapped in Al foil, vacuum-sealed in silica glass tubes and irradiated for 14 h at the B-1 CLICIT facility at the Radiation Center, Oregon State University, USA. Sample and flux monitor irradiation geometry followed those of Vasconcelos (1999). After a 2-month cooling period, two to four grains for each sample were analysed by the laser incremental heating $^{40}Ar/^{39}Ar$ method at the UQAGES laboratory. Irradiation correction factors are $(2.64\pm0.02)\times10^{-4}$ for $(^{36}Ar/^{37}Ar)_{Ca}$; $(7.04\pm0.06))\times10^{-4}$ for $(^{39}Ar/^{37}Ar)_{Ca}$; $(8\pm3)\times10^{-4}$ for $(^{40}Ar/^{39}Ar)_K$. A J factor of 0.003644 ± 0.000024 for the irradiation was calculated from the analysis of 15 individual sanidine flux monitor grains. Plateaus, defined as three or more contiguous steps accounting for more than 50% of the total amount of ^{39}Ar released from each sample, were used to calculate plateau ages (1 sigma error). All ages are reported using the constants of Steiger and Jäger (1977).

Major element oxides (wt.%) were determined using a Varian Vista PRO ICP-AES at the Key Laboratory of Isotope Geochronology and Geochemistry, Guangzhou Institute of Geochemistry, Chinese Academy of Sciences. The details of the analytical procedures were described by Li et al. (2002a). Trace elements, including the rare earth elements (REE), were analyzed using a Perkin-Elmer ELAN 6000 inductively-coupled plasma source mass spectrometer (ICP-MS) at the Key Laboratory of Isotope Geochronology and Geochemistry, Guangzhou Institute of Geochemistry, Chinese Academy of Sciences, following procedures described by Li et al. (2002a). Analytical precision for most elements is better than 3%.

Sr and Nd isotopic compositions for some samples were determined using a Finnigan MAT-262 mass spectrometer at the Institute of Geology and Geophysics, Chinese Academy of Sciences, Beijing, following procedures similar to those of Zhang et al. (2002). The $^{87}Sr/^{86}Sr$ ratio of NBS987 standard and the $^{143}Nd/^{144}Nd$ ratio of the La Jolla standard measured during the period of analysis were 0.710234 ±7 (2σm) and $^{143}Nd/^{144}Nd=0.511838\pm8$ (2σm), respectively. Sr and Nd isotopic compositions of other samples were measured by a Micromass Isoprobe multi-collector mass spectrometer (MC-ICP-MS) at the Guangzhou Institute of Geochemistry, Chinese Academy of Sciences. Analytical procedures are similar to that described by Wei et al. (2002) and Li et al. (2004). The $^{87}Sr/^{86}Sr$ ratio of the NBS987 standard and $^{143}Nd/^{144}Nd$ ratio of the JNdi-1 standard measured were 0.710288 ± 28 (2σm) and 0.512109 ± 12 (2σm), respectively. All measured $^{143}Nd/^{144}Nd$ and $^{86}Sr/^{88}Sr$ ratios are fractionation corrected to $^{146}Nd/^{144}Nd=0.7219$ and $^{86}Sr/^{88}Sr=0.1194$, respectively.

4. Results

Lavas of the Duogecuoren area include both adakitic and shoshonitic suites, based on petrological criteria and geochemical data. The adakitic rocks can be further subdivided into peraluminous and metaluminous subtypes (Fig. 2a). Both subtypes have similarities with slab-derived adakites, including high Sr (367–2472 ppm) and Al_2O_3 (14.55–16.86 wt.%) and low Y (3.05–16.9 ppm) and Yb (0.31–1.48 ppm) contents combined with high La/Yb (27–100) and Sr/Y (48–

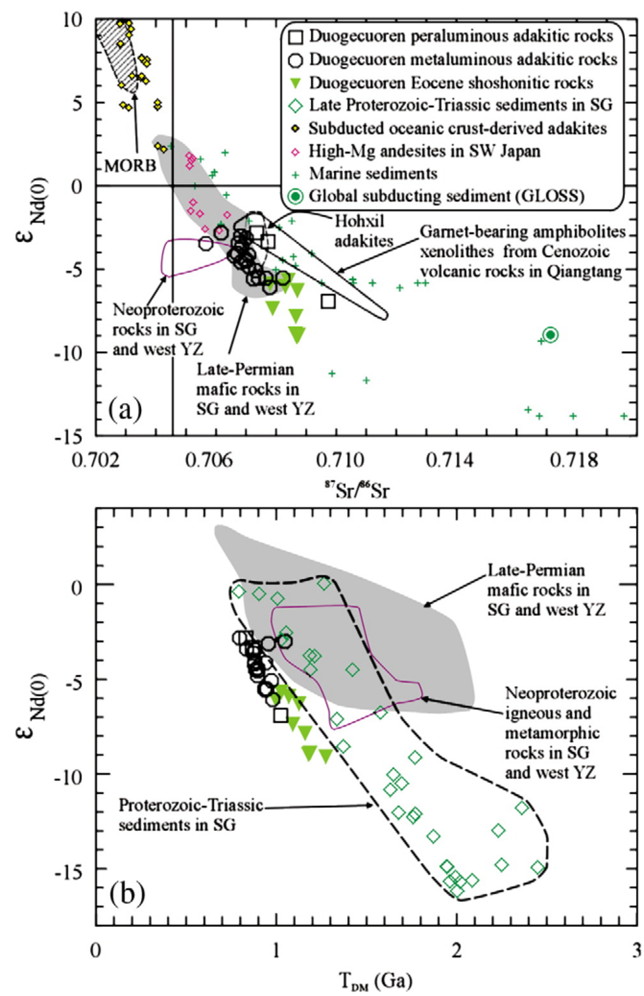

Fig. 5. (a) Nd–Sr and (b) Nd isotope diagrams for the Duogecuoren adakitic rocks. Cenozoic subducting oceanic crust-derived adakitic rocks are after Defant et al. (1992), Kay et al. (1993), and Stern and Kilian (1996). The data for the Duogecuoren shoshonitic rocks are from unpublished data of Q. Wang. The data for high-Mg andesites in SW Japan are from Shimoda et al. (1998). The data for garnet-bearing amphibolites xenoliths from Cenozoic volcanic rocks in Qiangtang are from Deng et al. (1998). The data for the Neoproterozoic igneous and metamorphic rocks in the Songpan-Ganzi and west Yangtze Blocks are from Roger and Calassou (1997) and Li et al. (2003). Proterozoic–Triassic sediments in the Songpan-Ganzi Block are from Chen et al. (2006) and She et al. (2006). Other data (e.g., the Hohxil adakitic rocks, Ulugh Muztagh rhyolites, Late Permian mafic rocks in SG west YZ, marine sediments and GLOSS) are the same as in Fig. 4.

240) ratios (see Appendix A; Fig. 2b) (Defant et al., 1990, 2002), negligible to positive Eu and Sr anomalies, and Nb, Ta and Ti depletion (Fig. 3a and b). The peraluminous adakitic rocks mainly contain phenocrysts of plagioclase, K-feldspar, quartz, magnetite and minor biotite, and are geochemically characterized by relatively high SiO_2 (>66 wt.%) contents (Fig. 2a), and low MgO (<1.0 wt.%), Cr (4.94–23.3 ppm) and Ni (2.33–17.0 ppm) contents, $Mg^{\#}$ (20–50) values (see Appendix A and Fig. 2c) and Nb/Ta ratios (Fig. 3c). Some samples plot in the field of syn-collisional granites (Fig. 2d). The metaluminous adakitic rocks contain phenocrysts of plagioclase, augite, hornblende, magnetite and minor K-feldspar ± olivine and microcrystals of feldspar and augite in the matrix. They are geochemically characterized by relatively low SiO_2 (55–69 wt.%) (Fig. 2a), and high MgO (1.41–6.34 wt.%), Cr (25.7–383 ppm), Ni (14.13–183 ppm) and $Mg^{\#}$ (46–69) values (see Appendix A), similar to slab-derived adakites or high-Mg andesites (Fig. 2c). They also exhibit higher Nb/Ta ratios than the peraluminous rocks (Fig. 3c). All samples of metaluminous adakitic rocks plot in the field of arc granites (Fig. 2d).

However, the Duogecuoren peraluminous and metaluminous adakitic rocks are different from slab-derived adakites in that: (a) some of them are peraluminous whereas slab-derived adakites are mainly metaluminous (Fig. 2a); (b) they have much higher K_2O (2.45–5.08 wt.%) and Th (11.2 to 32.3 ppm) contents and Th/La (0.23–0.88) ratios than slab-derived adakites (Fig. 4); (c) they have lower ε_{Nd} (−2.81 to −6.91) and higher $^{87}Sr/^{86}Sr$ (0.7057–0.7097) values than slab-derived adakites (see Appendix A and Fig. 5).

They are also clearly different from Late Mesozoic (Jurassic–Cretaceous) magmatic rocks, which are similar to "normal" arc andesite–dacite–rhyolite, in that they display high Y and heavy rare earth element contents, low Sr/Y ratios and clearly negative Eu and Sr anomalies (Figs. 2b and 3a and b). The Duogecuoren adakitic lavas are also different from the Bandaohu shoshonitic lavas (Fig. 1b) in that the latter contain phenocrysts of K-feldspar, hornblende, magnetite and minor plagioclase, quartz and biotite, and exhibit much higher K_2O (Fig. 4a) and almost all trace element contents (Figs. 2c and 3a and b).

The data for SHRIMP U–Pb zircon, $^{40}Ar/^{39}Ar$, and LAM-ICP-MS U–Pb zircon dating are listed in Appendices C–G. The results of SHRIMP U–Pb zircon analyses for two samples (metaluminous (5144-1) and peraluminous (D2390) adakitic rocks) are illustrated on a concordia plot in Fig. 6a–c. The 11 analyses for sample 5144-1 and 13 analyses for sample D2390 define single age populations with a weighted mean $^{206}Pb/^{238}U$ age of 44.3 ± 1.8 Ma (2σ) (MSWD = 3.0) and 41.96 ± 0.73 Ma (2σ) (MSWD = 1.03), respectively (Fig. 6a–c). The results of $^{40}Ar/^{39}Ar$ dating for 12 analyses from 9 other samples of (high MgO) metaluminous adakitic rocks exhibit ages ranging from 45.69 ± 0.16 to 37.60 ± 0.16 Ma (Figs. 7 and 8). Thus, the Duogecuoren adakitic rocks were formed in the Eocene (46–38 Ma). In addition, the LA-ICP-MS U–Pb zircon results for sample 8524-1 of the Bandaohu shoshonitic rocks establish an age of 40.18 ± 0.39 Ma (Fig. 6d), similar to the formation age of adakitic rocks. Therefore, apart from ~3 Ma lavas in the northern Dongyuehu area (Fig. 1b) (Hacker et al., 2000), the adakitic and

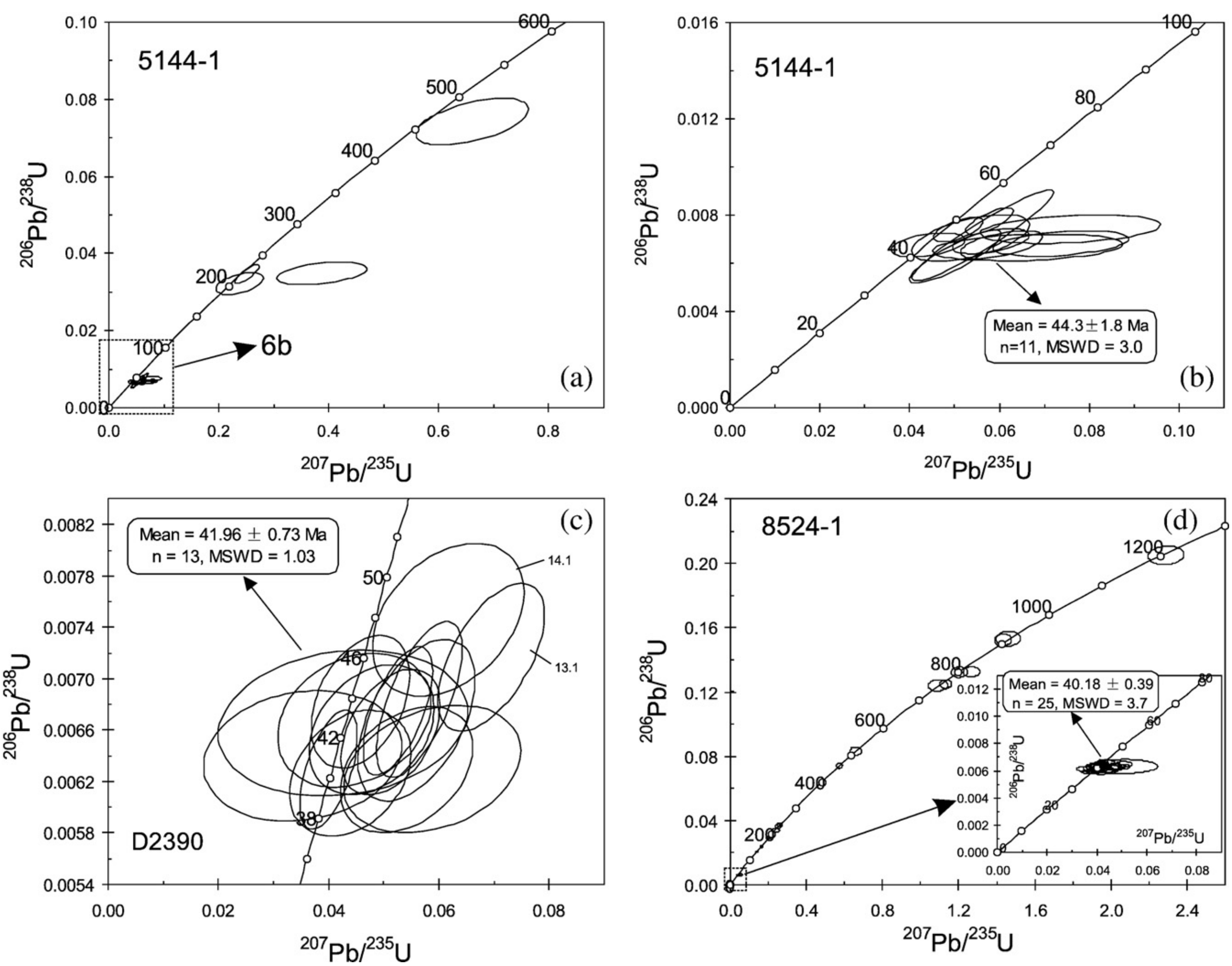

Fig. 6. SHRIMP zircon (a–c) and LA-ICP-MS U–Pb (d) concordia diagrams for Samples 5144-1, D2390 and 8524-1.

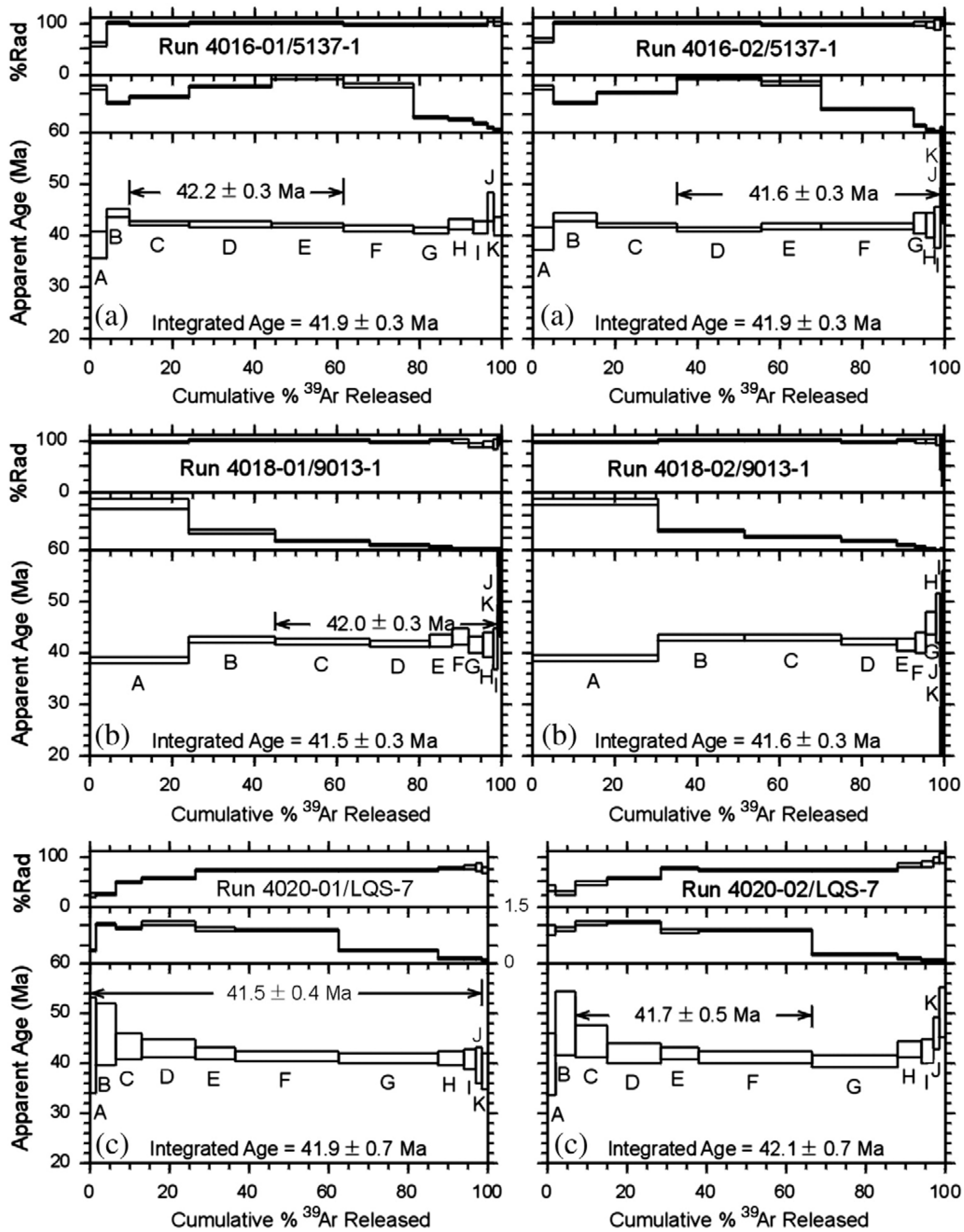

Fig. 7. Incremental-heating spectra for 2 replicate grains from the 3 samples from the Duogecuoren high-Mg adakitic rocks. (a) The two grains analysed for Sample 5137-1 yield reproducible plateaus (42.2±0.3 and 41.6±0.3). A probability density plot for the two grains yields a maximum probability peak at 42.0 Ma and defines a mean-weighted age of 41.8±0.3 Ma when all outliers are eliminated. An isochron for both grains yields an age of 41.9±0.3 Ma, with a $^{40}Ar/^{36}Ar$ intercept of 254±10 Ma. (b) One of two grains analysed for Sample 9013-1 yields a plateau (42.0±0.3). A probability density plot for both grains yields a maximum probability peak at 42.0 Ma and defines a mean-weighted age of 42.5±0.4 Ma when all outliers are eliminated. An isochron for the two grains yields an age of 42.9±0.3 Ma, with a $^{40}Ar/^{36}Ar$ intercept of 340±90 Ma. (c) The two grains analysed for Sample LQS-7 yield the plateaus (41.5±0.4 and 41.7±0.5). A probability density plot for both grains yields a maximum probability peak at 41.3 Ma and defines a mean-weighted age of 41.5±1.1 Ma when all outliers are eliminated. An isochron for both grains yields an age of 41.5±0.4 Ma, with a $^{40}Ar/^{36}Ar$ intercept of 308±4 Ma.

shoshonitic lavas in the Duogecuoren area were mainly erupted in the Middle Eocene (46–38 Ma).

5. Discussion

5.1. Previous models for the petrogenesis of adakitic rocks

A variety of origins have been proposed for adakitic rocks: (a) melting of subducted oceanic crust, followed by interaction with the overlying mantle wedge (e.g., Stern and Kilian, 1996; Rapp et al., 1999; Defant et al., 2002; Zhou et al., 2006b; Wang et al., 2007a, 2008); (b) high-pressure fractional crystallization (involving garnet) of hydrous basaltic melts (Prouteau and Scaillet, 2003; Macpherson et al., 2006); (c) crustal assimilation and low pressure fractional crystallization (involving olivine+clinopyroxene+plagioclase+hornblende+titanomagnetite) process from parental basaltic magmas (Castillo et al., 1999); (d) mixing of felsic and basaltic magmas (Streck et al., 2007); (e) melting of thickened mafic lower continental crust (e.g., Atherton and Petford, 1993; Hou et al., 2004; Chung et al., 2005; Wang et al., 2005, 2007b; Zhang et al., 2006); and (f) melting of delaminated lower crust (Kay and Kay, 1993; Xu et al., 2002; Gao et al., 2004; Wang et al., 2006). The tectonic setting and the geochemical and mineralogical characteristics of the Duogecuoren adakitic rocks can be used to rule out the six hypotheses.

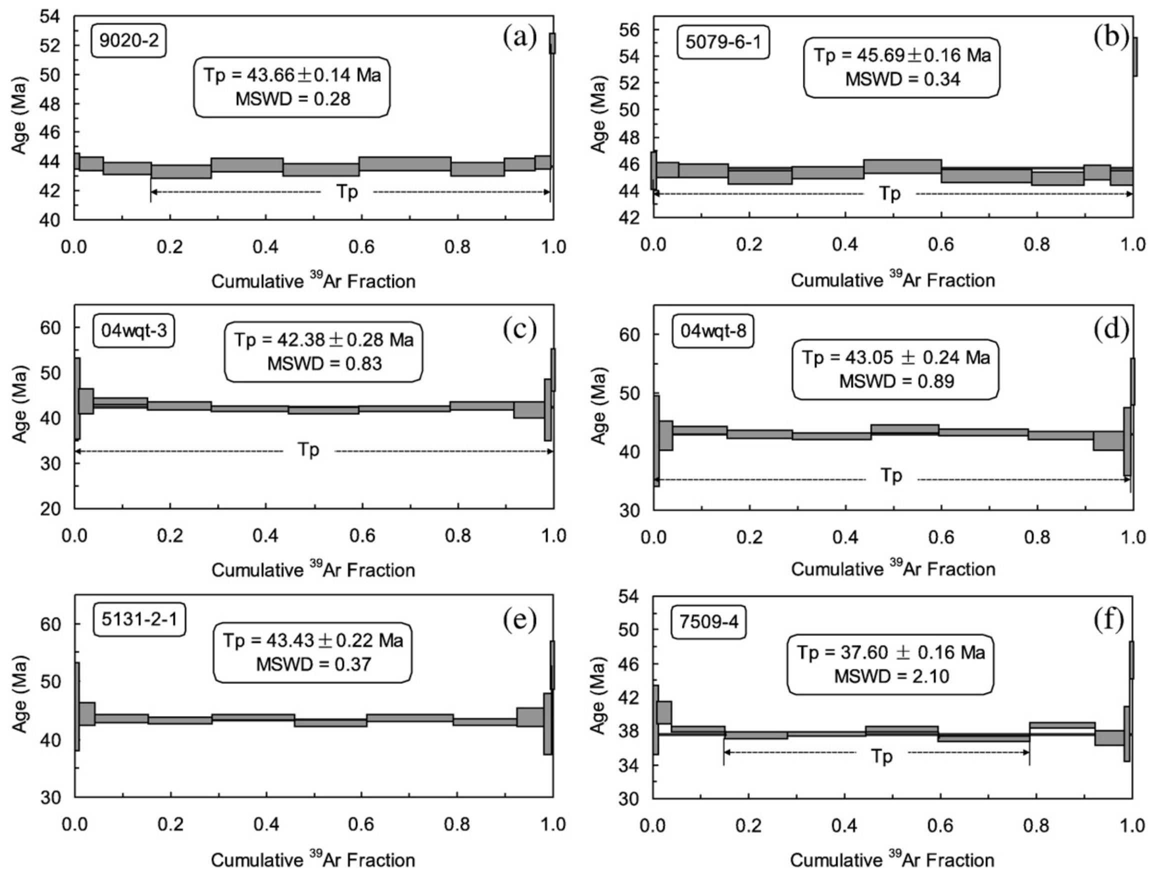

Fig. 8. The $^{40}Ar/^{39}Ar$ age spectra diagrams for the Duogecuoren adakitic rocks.

The possibility that melting of subducted Neotethyan oceanic crust generated the Duogecuoren adakitic rocks can be ruled based on their geochemical characteristics and the tectonic context of the Qiangtang Block in the Eocene. Commonly, adakites from modern arcs that are interpreted as slab melts have mid-ocean-ridge basalt (MORB)-like Sr–Nd isotopic compositions and relatively low K_2O, Th and Th/La values, which originate from the basaltic portion of subducting slabs (Figs. 4 and 5) (Defant and Drummond, 1990; Kelemen et al., 2003; Plank, 2005). In contrast, the Duogecuoren adakitic rocks have more evolved isotopic compositions (Fig. 5) and much higher K_2O, Th and Th/La values (Fig. 4), indicating that their source rocks were not basaltic oceanic crust. Additionally, since the Middle Cretaceous when the suturing of the Songpan-Ganzi–Qiangtang and Qiangtang–Lhasa blocks occurred (Yin and Harrison, 2000), the Qiangtang Block has been in an intra-continental setting. Even if as much as 1500 km of crustal shortening took place in the Cenozoic (Molnar and Tapponnier, 1975), then the Duogecuoren area remained much more than 500 km away from the Indus Suture from the Eocene to the present (Fig. 1a). Thus, flat subduction of Neotethyan oceanic crust beneath the Qiangtang Block in Eocene would be required. However, no geophysical data support such a scenario (e.g., Kind et al., 2002; Molnar and Tapponnier, 1975; Tapponnier et al., 2001). Moreover, the close proximity of large-scale Cretaceous–Early Tertiary arc magmatic rocks in southern Tibet to the Indus suture (Fig. 1a) implies that prior to continental collision, oceanic lithosphere did not descend into the asthenosphere beneath Tibet at an unusually shallow angle (Molnar and Tapponnier, 1975). The Neotethyan slab is more likely to have become detached from the orogenic system in southern Tibet and then to have sunk into the deep mantle in Eocene time (DeCelles et al., 2002; Kohn and Parkinson, 2002).

The high-pressure fractional crystallization (involving garnet) of hydrous basaltic melts could not generate the Duogeguoren adakitic rocks. Suites of adakitic rocks derived by high-pressure fractional crystallization involving garnet will generally display distinct geochemical trends (Macpherson et al., 2006). In such suites, the Al_2O_3 and La contents decrease with the increasing of SiO_2 contents (Fig. 9a–b), and La/Y, Dy/Yb and Sr/Y ratios clearly increase with the increasing of SiO_2 contents (Fig. 9c–e). However, the Duogeguoren adakitic rocks exhibit none of these trends (Fig. 9a–e). Moreover, the only coeval basaltic rocks associated with the Eocene adakitic rocks are very minor mafic shoshonitic occurrences, which cannot be linked to the adakitic rocks by fractional crystallization garnet (Fig. 9a–j).

The Duogecuoren adakitic rocks were also not derived from parental basaltic magmas by crustal assimilation and low pressure fractional crystallization. The Duogecuoren adakitic rocks do not exhibit the compositional trends produced by low pressure fractional crystallization of a hornblende-bearing assemblage in Fig. 9a–b and f–i. The high SiO_2-peraluminous adakitic rocks have much lower Y and HREE contents than the low SiO_2-metaluminous adakitic rocks, which is also not in agreement with the crystal fractionation trend of olivine (Ol)+plagioclase (Pl)+clinopyroxene (Cpx)+orthopyroxene (Opx) (Fig. 2b). Moreover, both high SiO_2-peraluminous and low SiO_2-metaluminous adakitic rock samples have similar Sr–Nd isotopic compositions, mainly with higher $\varepsilon_{Nd}(0)$ and lower $^{87}Sr/^{86}Sr$ values than shoshonitic rock samples (Figs. 5 and 9j–k), which is inconsistent with a crustal assimilation model. A SiO_2 versus $Mg^{\#}$ diagram (Fig. 2c) illustrates that the range of adakitic rock compositions are also inconsistent with the trend of crustal assimilation and fractional crystallization (AFC) processes.

Mixing of dacitic and basaltic magmas was recently proposed for the genesis of some high-Mg and low SiO_2 adakitic rocks, whose high Sr/Y and overall adakite affinity may be inherited from a dacite end member of crustal origin (Streck et al., 2007). A similar process in the Duogecuoren area would require that the high-Mg and low SiO_2

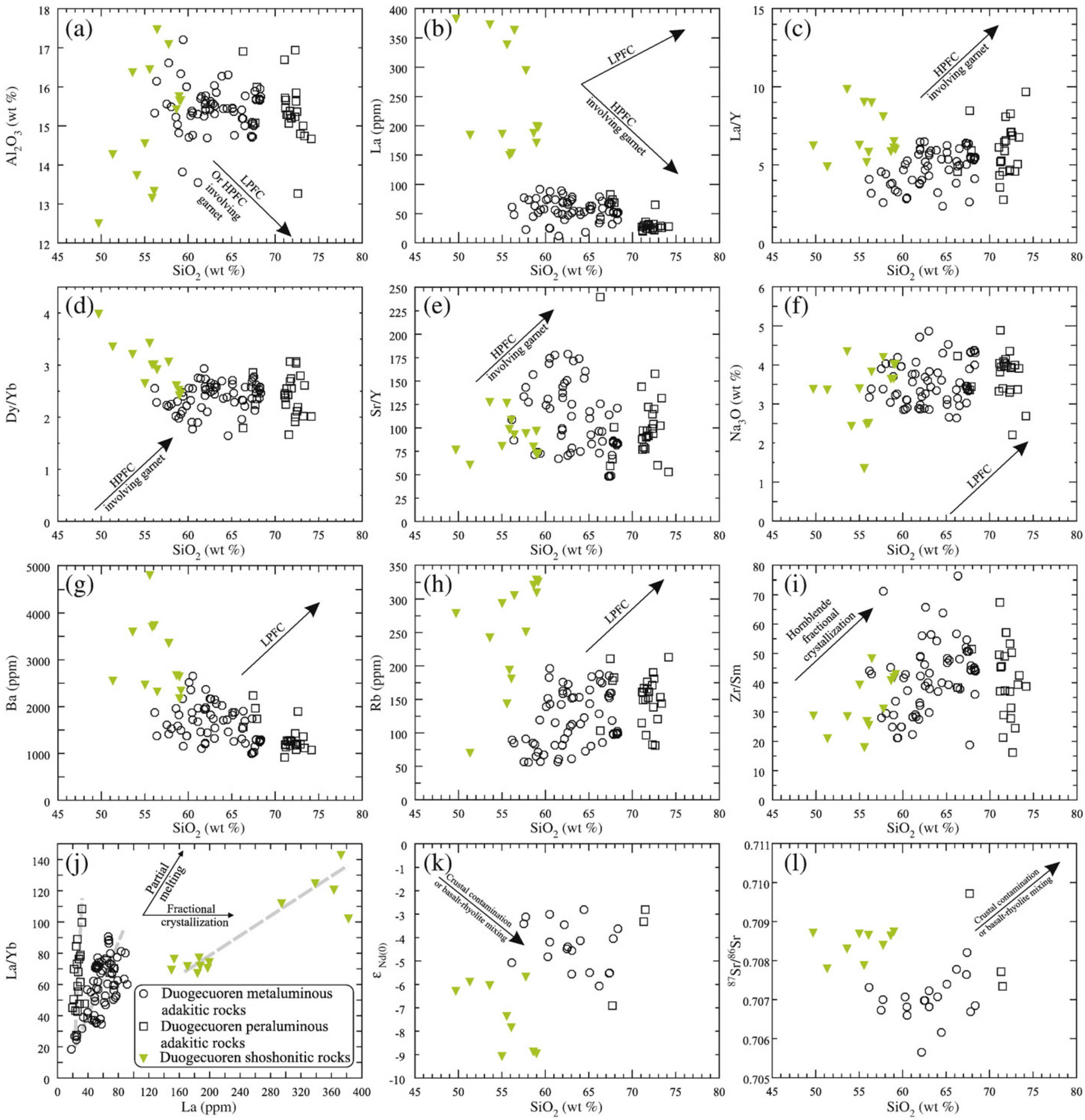

Fig. 9. (a) SiO_2 versus Al_2O_3; (b) SiO_2 versus La; (c) SiO_2 versus La/Y; (d) SiO_2 versus Dy/Yb; (e) SiO_2 versus Sr/Y; (f) SiO_2 versus Na_2O; (g) SiO_2 versus Ba; (h) SiO_2 versus Rb; (i) SiO_2 versus Zr/Sm; (j) La versus La/Yb; (k) SiO_2 versus $e_{Nd}(0)$; (l) SiO_2 versus $^{87}Sr/^{86}Sr$. Fractional crystallization trends in a–h: HPFC, high-pressure fractional crystallization involving garnet (Macpherson et al., 2006); LPFC, low pressure fractional crystallization involving olivine + clinopyroxene + plagioclase + hornblende + titanomagnetite (Castillo et al., 1999). Due to the incompatibility of Zr and compatibility of Sm in hornblende (Drummond et al., 1996), the fractional crystallization will cause the increasing of Zr/Sm ratios in residual magmas (i). Fractional crystallization and partial melting trends in j are after Turner et al. (1996). The data for the Duogecuoren shoshonitic rocks are from unpublished data of Q. Wang. The data for the Duogecuoren adakitic rocks are from Appendix A and unpublished data of Y. Dong.

metaluminous adakitic rocks were derived by the mixing of the dacitic to rhyolitic peraluminous adakitic magmas and shoshonitic magma, which represents the only candidate for a mantle-derived mafic end member. Several factors suggest this model is highly unlikely. First, magma mixing should produce straight arrays in binary plots (Macpherson et al., 2006), but K_2O, Al_2O_3, La and Rb versus SiO_2 plots (Figs. 4a, and 9a–b, h) do not display such straight arrays. Secondly, the high-Mg and low SiO_2 metaluminous adakitic rocks in the Duogecuoren area have Dy/Yb, Sr/Y and La/Yb ratios that are similar to the low-Mg and high SiO_2 peraluminous adakitic rocks (Fig. 9d, e, j), indicating that their adakite affinity is not inherited from the dacite–rhyolite end member. Finally, the shoshonitic rocks have lower $e_{Nd}(0)$ and higher $^{87}Sr/^{86}Sr$ values than most high-Mg and low-Mg adakitic rocks, indicating that the shoshonitic and dacitic–rhyolitic magmas cannot be two end members in a magma mixing scenario (Fig. 9k, l).

There is a possibility that the high SiO_2-peraluminous adakitic rocks were generated by melting of thickened mafic lower continental crust owing to their relatively low-MgO or -Mg# values (Fig. 2c), and Cr and Ni contents. However, the low SiO_2-metaluminous adakitic rocks cannot originate by this mechanism, as they have higher Mg# values than metabasaltic and eclogite experimental melts (1–4.0 GPa) (Rapp et al., 1999, 2003). In fact, some samples have very high Cr and Ni contents and contain olivine phenocrysts.

Some intra-continental high-MgO or -Mg# adakitic rocks have been considered to originate from the melting of delaminated lower crust (e.g., Xu et al., 2002; Gao et al., 2004; Wang et al., 2006). Although the model seems applicable to the Duogecuoren metaluminous adakitic rocks, it is not supported by evidence from xenoliths in Cenozoic volcanic rocks or by structural studies. As detailed in numerous studies, xenolith compositions suggest that the northern Qiangtang has a dominantly sedimentary lower crust formed from subducted Triassic Songpan-Ganzi accretionary wedge rocks in the Early Mesozoic or Cenozoic (Hacker et al., 2000, 2005; Yin and Harrison, 2000; Kapp et al., 2003, 2005; Schwab et al., 2004). Obviously, this sedimentary lower crust has a lower density than mantle rocks at the same pressure and temperatures (Hacker et al., 2005), which is not favourable for the delamination of lower crust. Moreover, within a continent, the delamination of lower crust is generally restricted to such regions that are undergoing extension, are underlain by a mantle plume, or have had part of the conductive upper mantle removed (Jull and Kelemen, 2001; Wang et al., 2007b). In fact, several examples of adakitic rocks derived by melting of delaminated lower crust have been documented in regions that were characterized by lithospheric extension (Xu et al., 2002; Gao et al., 2004; Wang et al., 2006). In contrast, the presence of thrust faults (Fig. 1a) and contraction basins suggests that the Qiangtang Block was undergoing crustal shortening during the Paleocene–Early Miocene (Yin and Harrison, 2000; Tapponnier et al., 2001; Wang et al., 2002; Kapp et al., 2005; Spurlin et al., 2005). Accordingly, it seems unlikely that the delamination of lower crust took place in the Qiangtang Block in the Eocene.

5.2. A new model for the petrogenesis of the Duogecuoren adakitic rocks

We propose an alternative model for the Duogecuoren adakitic rocks (Fig. 10), given that crustal shortening in this area most plausibly required continental subduction as the major accommodation mechanism (Yin and Harrison, 2000; Tapponnier et al., 2001; Ding et al., 2003; Kapp et al., 2005). The continental subduction could have been either south-dipping along the Jinsha suture (Meyer et al., 1998; Roger et al., 2000; Yin and Harrison, 2000; Tapponnier et al., 2001; Ding et al., 2003) or north-dipping along the Bangong suture (Kapp et al., 2003, 2005; Spurlin et al., 2005). The latest geophysical data, however, support south-dipping continental subduction along both the Jinsha suture (Tapponnier et al., 2001; Kind et al., 2002; Vergne et al., 2002; Kumar et al., 2006; Wittlinger et al., 2004) and the Bangong suture (Shi et al., 2004). Thus, Eocene lavas in the northern Qiangtang Block (Fig. 1a) were most likely related to the south-dipping continental subduction along the Jinsha suture (Meyer et al., 1998; Hacker et al., 2000; Roger et al., 2000; Tapponnier et al., 2001) rather than convective thinning of the mantle lithosphere (Chung et al., 1998) or back-arc extension (Chung et al., 2005). Priestley et al. (2006) find that high-velocity material underlies most and possibly all of Tibet to a depth of 225–250 km and suggest that the Indian lithosphere has not detached and sunk beneath the plateau but that most of the plateau has been underthrust by high-velocity Indian mantle from the south and possibly high-velocity Asian mantle from the north. Petrogenesis of Cenozoic shoshonitic lavas in the Qiangtang Black has generally been ascribed to the melting of enriched lithospheric mantle, which was initiated by continental subduction (e.g., Hacker et al., 2000; Yin and Harrison, 2000; Tapponnier et al., 2001; Wang et al., 2001; Ding et al., 2003; Spurlin et al., 2005). The Duogecuoren adakitic rocks differ geochemically from coeval shoshonitic rocks (Figs. 2b, 3a and b and 4a) and clearly reflect a distinct petrogenetic mechanism. As the Songpan-Ganzi Block likely subducted along the Jinsha suture beneath the northern Qiangtang Block during the Paleocene–Early Miocene (e.g., Hacker et al., 2000; Tapponnier et al., 2001), we suggest that the adakitic rocks were most probably derived by melting of continental crust from the southward subducted Songpan-Ganzi Block.

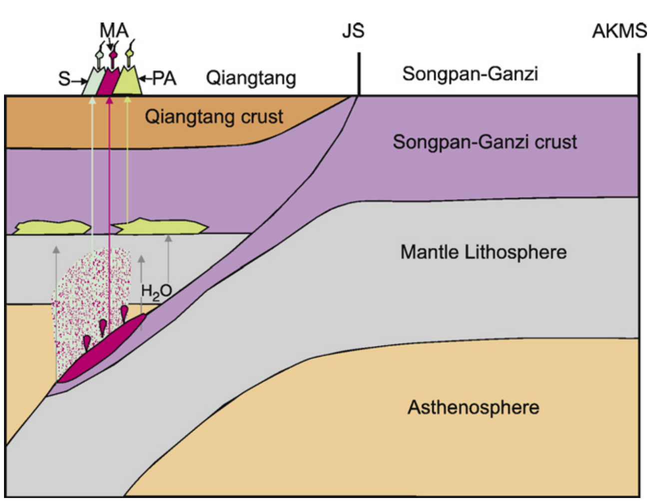

Fig. 10. A suggested model to produce Eocene igneous rocks in the Northern Qiangtang area (modified from Yin and Harrison (2000), Tapponnier et al. (2001), Kapp et al. (2005) and Ding et al. (2007)). S—shoshonitic rocks; MA—metaluminous adakitic rocks; PA—peraluminous adakitic rocks; suture: AKMS—Anyimaqen–Kunlun–Muztagh; JS—Jinshajiang.

The Songpan-Ganzi Block consists of Triassic flysch (Yin and Harrison, 2000) and some Late Permian basaltic and Proterozoic rocks (Roger and Calassou, 1997; Song et al., 2004; Wang, 2005; Xiao and Xu, 2005). The Duogecuoren adakitic rocks exhibit Nd–Sr isotopic compositions similar to Late Permian basaltic rocks in the Songpan-Ganzi Block or west Yangtze Block (Xu et al., 2001; Song et al., 2004), and are partially similar to Proterozoic rocks in the Songpan-Ganzi Block or west Yangtze Block (Roger and Calassou, 1997; Li et al., 2003) (Fig. 5). However, these Late Permian basaltic and Proterozoic rocks display much lower Th and Th/La values than the Duogecuoren adakitic rocks (Fig. 5), indicating that the Duogecuoren adakitic rocks were not derived from an entirely comparable source but from one that must also have a high Th and Th/La component (Fig. 4b). Recently published isotopic studies (Chen et al., 2006; She et al., 2006) demonstrate that Proterozoic–Triassic sediments in the Songpan-Ganzi Block, including Triassic flysch, have a wide range of $\varepsilon_{Nd}(0)$ values (−0.37 to −15.68), which overlays that of Eocene adakitic rocks (−2.81 to −6.91) in the Duogecuoren area (Fig. 5b). Furthermore, we note that the Duogecuoren adakitic rocks, especially the peraluminous adakitic rocks, are geochemically similar to marine sediments. For example, all samples for the Duogecuoren adakitic rocks plot in the field of marine sediments in the Nd–Sr isotopic diagram (Fig. 5). They also exhibit high K_2O, Th and Th/La values similar to these marine sediments or to the upper continental crust (Fig. 4) (Condie, 1993; Plank and Langmuir, 1998; Plank, 2005, and references therein), indicating that their source likely contained sediments (Plank and Langmuir, 1993; Hawkesworth et al., 1997; Plank, 2005;). For example, experimental results indicate that, in a subduction zone, Th enrichment with respect to MORB requires sediment melting (Johnson and Plank, 1999).

Xenoliths of garnet-bearing amphibolites, granulites and eclogites from Cenozoic volcanic rocks in Qiangtang and Pamir areas are considered to have been derived from mafic or sedimentary rocks of subducted continental crust (Hacker et al., 2000, 2005). The granulites from 3-million-year-old Ma shoshonitic volcanic rocks in the northern Dongyuehu area (Fig. 1b) were probably residue after low-grade sediments such the Songpan-Ganzi flysch melted during early introduction to the deep crust (Hacker et al., 2000). Moreover, REE patterns of the Duogecuoren adakitic rocks are similar to those of melt derived from metapelitic granulite or melt inclusions from quartz crystals in metapelitic granulite in the Pamir (Fig. 3a) (Hacker et al., 2005). Therefore, we suggest that the melting of subducted continental sediments may have played an important role in the petrogenesis of the Duogeguoren adakitic rocks.

Dehydration melting experiments for metasedimentary rocks suggest that their melts at high pressure (1–4 GPa) are peraluminous with low $Mg^{\#}$ (<47) (e.g., Castro et al., 2000; Schmidt et al., 2004). Accordingly, only the peraluminous and low-$Mg^{\#}$ adakitic rocks in the Duogecuoren area could be generated directly from subducted sediments. The metaluminous and high-$Mg^{\#}$ adakitic rocks are similar to the high-Mg andesites in SW Japan in terms of ACNK (Al_2O_3/(CaO+Na_2O+K_2O), $Mg^{\#}$, Rb, Y+Nb, Th/La values and Nd–Sr isotopic compositions. The Japanese high-Mg andesites resulted from the reaction between subducted sediment-derived melts and mantle (Shimoda et al., 1998; Tatsumi, 2001; Tatsumi and Hanyu, 2003). A sediment-derived melt changes its composition from rhyolite to andesitic as it dissolves olivine and clinopyroxene and crystallizes orthopyroxene (Tatsumi, 2001). Therefore, we argue that the metaluminous and high-$Mg^{\#}$ adakitic rocks in the Duogecuoren area most probably resulted from reaction between ascending melts derived from subducted sediment-dominated continental crust and mantle peridotite. However, this mechanism for the generation of high-$Mg^{\#}$ adakitic rocks is clearly different from those which generate high-$Mg^{\#}$ adakitic rocks or andesites by reaction between ascending melts derived from delaminated lower crust (Xu et al., 2002; Gao et al., 2004; Wang et al., 2006) or subducted oceanic sediments or crust and mantle peridotite (Kelemen, 1995; Stern and Kilian, 1996; Shimoda et al., 1998; Rapp et al., 1999; Tatsumi, 2001; Defant et al., 2002; Tatsumi and Hanyu, 2003).

Although sediment melting models have primarily been applied to arc settings involving subduction of oceanic crust containing sediments (Johnson and Plank, 1999; Plank, 2005, and references therein), they should also be applicable to the subduction of continental crust containing sediments (e.g., the Songpan-Ganzi Block). In addition to Middle–Late Permian basalts, which are similar to contemporaneous plume-related basalts in the western Yangtze and the eastern margin of Tibet (Song et al., 2004; Wang, 2005; Xiao and Xu, 2005), the Songpan-Ganzi Block also contains the world's largest accumulation of Triassic sediments. They partially cover the earlier basalts and mainly consist of flysch. Following the Eocene (~55 Ma) collision of India with Asia (Molnar et al., 1993; Tapponnier et al., 2001), the Songpan-Ganzi Block subducted southward beneath the Qiangtang Block along the reactivated Triassic Jingsha suture (Tapponnier et al., 2001; Kind et al., 2002; Vergne et al., 2002; Kumar et al., 2006) (Fig. 1a). During subduction of the Songpan-Ganzi Block, the basaltic layer underlying Triassic sediments began to dehydrate under eclogite facies conditions. As sediments have a relatively low solidus (H_2O+Cl fluid-saturated) at high pressure (775±25 °C at 2 GPa: Johnson and Plank, 1999), the ascending fluids triggered melting of sediment-dominated continental crust, which generated K-rich and peraluminous melts (Johnson and Plank, 1999; Schmidt et al., 2004). The relatively low zircon saturation temperatures (Tzr) (611–793 °C) (Miller et al., 2003) (Appendix A) for both peraluminous and metaluminous adakitic rocks further support the above inference. Adakitic liquids can generally be produced by melting of mafic materials at pressures equivalent to a crustal thickness of >50 km where the residual phases include garnet±rutile but little or no plagioclase (Rapp et al., 1999, 2003; Kay and Kay, 2002; Xiong et al., 2005; Xiao and Clemens, 2007). Pelitic sediments and greywackes have the same eclogitic mineralogy (but different mineral proportions) as basaltic rocks at depths>70–100 km (i.e., 2.0–3.5 GPa: Schmidt et al., 2004). Experimental data suggest that sediment-dominated melts in equilibration with garnet are markedly depleted in HREE and enriched in LREE (Johnson and Plank, 1999).

Melts derived from sediment-dominated continental crust of the Songpan-Ganzi Block should have similar REE characteristics. Those melts mainly generated at a relatively shallow depth (the hornblende+garnet stability field: Condie, 2005; Foley et al., 2002; Fig. 3c) did not interact significantly with mantle and ascended to form the low MgO and peraluminous adakitic rocks (Fig. 10). Melts mainly generated at greater depths (the garnet+rutile stability field: Condie, 2005; Xiong et al., 2005; Fig. 3c) interacted with mantle peridotite: (a) MgO and compatible elements (e.g., Cr and Ni) entered into some melts, which caused the formation of the high MgO and metaluminous adakitic rocks (Fig. 10); (b) some melts or fluid metasomatized the mantle, which created source regions for ultrapotassic (or shoshonitic) magmas (e.g., Schmidt et al., 2004) (Fig. 10).

5.3. Implications

Geophysical data reveal that the crustal thickness of the Qiangtang Block is ~70–90 km, corresponding to a Central Tibetan Plateau surface elevation≥4.5 km above sea level (Tapponnier et al., 2001; Kind et al., 2002; Vergne et al., 2002; Wittlinger et al., 2004; Priestley et al., 2006). However, the timing and mechanism of its uplift remain at issue (Molnar et al., 1993; Turner et al., 1996; Yin and Harrison, 2000; Tapponnier et al., 2001; Kohn and Parkinson, 2002; Chung et al., 2005; Harris, 2006). For example, some research suggests that the eruption of Eocene shoshonitic lavas in the east Qiangtang Block had no topographic implications for the Tibetan Plateau (Kohn and Parkinson, 2002) or that uplift of the Qiangtang plateau may have been initiated in the east from the Oligocene–Miocene (Chung et al., 2005) rather than in the Eocene (Chung et al., 1998). Nonetheless, tectonic data and basin and deformation analysis indicate that crustal shortening and uplifting of the Qiangtang plateau could, in fact, have begun in the Eocene (e.g., Tapponnier et al., 2001; Spurlin et al., 2005; Zhou et al., 2006a). In addition, oxygen isotope data from Late Eocene deposits in the center of the Tibetan Plateau indicate that the surface of Tibet has been at an elevation of more than 4 km for at least the past 35 Ma (Rowley and Currie, 2006).

The Eocene adakitic rocks of the Duogecuoren area in the western Qiangtang Block provide additional independent constraints on the geodynamic history of the region. They are geochemically distinct from Late Mesozoic (Jurassic–Cretaceous) intermediate-acid igneous rocks, which have negative Eu anomalies and enriched HREE contents, indicating plagioclase but no garnet in their source (Fig. 3c). In other words, the adakitic rocks obviously originated from a much deeper source than the Late Mesozoic intrusions. The adakitic rocks were derived from the melting of eclogitic crust which was thickened by continental subduction. This relationship implies that uplift of Central Tibetan Plateau probably initiated as early as 45–38 Ma and was likely related to the Eocene subduction of Asian continental lithosphere (Yin and Harrison, 2000; Tapponnier et al., 2001; Kind et al., 2002; Kumar et al., 2006; Rowley and Currie, 2006).

In the past decade, the relationship between Cenozoic global climate change and the uplift of the Tibetan Plateau has attracted wide interest but has also been the subject of dispute (e.g., Harrison et al., 1992; Prell and Kutzbach, 1992; Raymo and Ruddiman, 1992; Molnar et al., 1993; Turner et al., 1996; Ruddiman, 1998; Chung et al., 2005; Harris, 2006; Dupont-Nivet et al., 2007). Many, probably most, researchers believe that global cooling in Late Cenozoic was caused by uplift of the Tibetan Plateau (e.g., Harrison et al., 1992; Prell and Kutzbach, 1992; Turner et al., 1996). Global climate change in the Miocene was considered to have been related to approximately contemporaneous (13–7 Ma) uplift of the Tibetan Plateau (Harrison et al., 1992; Prell and Kutzbach, 1992; Turner et al., 1996). However, oceanic O–Sr isotopic variations, global cooling and Asian continental aridification began in the Eocene (40–35 Ma) (Raymo and Ruddiman, 1992; Ruddiman, 1998; Dupont-Nivet et al., 2007). Based on the presence of shoshonitic igneous rocks in the eastern Qiangtang Block, Chung et al. (1998) argued that large-scale uplift occurred there as early as 37–33 Ma, thereby accounting for the tectonically driven models of oceanic strontium isotope evolution and global cooling (Raymo and Ruddiman, 1992; Ruddiman, 1998). Recently, however, Chung et al. (2005) refuted this position and argued that Eocene uplift of the east Qiangtang Block did not take place. Therefore, possible links between climate and uplift of the Tibetan Plateau have remained unclear. The unresolved question has been whether exploration of Tibet could reveal evidence of even earlier uplift, particularly during the interval of global cooling between 55 and 40 Ma (Ruddiman, 1998). It is therefore significant that our results suggest uplift of the Central Tibetan Plateau was initiated as early as 46–38 Ma, which provides important evidence for the tectonically driven models for O–Sr isotopic evolution in the ocean, global cooling and Asian continental aridification in Eocene.

6. Conclusions

(1) Most of the Duogecuoren lavas of the central-western Qiangtang Block are high-K calc-alkaline andesites, dacites and rhyolites, and geochemically similar to adakitic rocks derived by partial melting of an eclogitic source. They can be further classified as either peraluminous-low-MgO or metaluminous-high-MgO subtypes.
(2) ^{40}Ar–^{39}Ar and SHRIMP and LAM-ICP-MS zircon U–Pb dating suggest that both peraluminous and metaluminous adakitic rocks erupted in the Eocene (46–38 Ma).
(3) The peraluminous adakitic rocks were probably derived by partial melting of subducted sediment-dominated continental crust of the Songpan-Ganzi Block along the Jinsha suture to the north, but the metaluminous adakitic rocks likely originated from the interaction between subducted sediment-dominated continental crust-derived melts and mantle.
(4) Eocene continental subduction along the Jinsha suture caused the thickening of the Qiangtang crust. The elevation of the Central Tibetan Plateau probably began as early as 45–38 Ma ago.

Acknowledgments

We sincerely thank editor professor Claude P. Jaupart and two anonymous reviewers for their constructive and helpful reviews. Professor Liu Dunyi, Tao Hua, Zhang Yuhai, Li Zhongliang, Lin Shiliang, Ou Chunsheng, Zhou Banggong, Tian Yungui and Chen Zhenyu are thanked for their assistance with laboratory and fieldwork. Financial support for this research was provided by Chinese Academy of Sciences (KZCX3-SW-143 and KZCX2-YW-128), the National Natural Science Foundation of China (Grant Nos. 40572042, 40673037 and 40425003), and the International Development Fund of The University of Sydney. This is also contribution no. 524 from the ARC GEMOC National Key Centre (www.es.mq.edu.au/GEMOC/). This study used instrumentation (LAM-ICP-MS) funded by ARC LIEF and DEST Systemic Infrastructure Grants, Macquarie University and industry. It also used ARC funded instrumentation at UQAGES.

Appendix A. Supplementary data

Supplementary data associated with this article can be found, in the online version, at doi:10.1016/j.epsl.2008.04.034.

References

Andersen, T., 2002. Correction of common lead in U–Pb analyses that do not report ^{204}Pb. Chem. Geol. 192, 59–79.
Atherton, M.P., Petford, N., 1993. Generation of sodium-rich magmas from newly underplated basaltic crust. Nature 362, 144–146.
Blisniuk, P.M., Hacker, B.R., Glodny, J., Ratschbacher, L., Bi, S., Wu, Z., McWilliams, M.O., Calvert, A., 2001. Normal faulting in central Tibet since at least 13.5 Myr ago. Nature 412 (6847), 628–632.
Boynton, W.V., 1984. Cosmochemistry of the earth elements: meteorite studies. In: Henderson, R. (Ed.), Rare Earth Element Geochemistry: Developments in Geochemistry, vol. 2. Elsevier, Amsterdam, pp. 89–92.
Castillo, P.R., Janney, P.E., Solidum, R.U., 1999. Petrology and geochemistry of Camiguin island, southern Philippines: insights to the source of adakites and other lavas in a complex arc setting. Contrib. Mineral. Petrol. 134, 33–51.
Castro, A., Guiliermo Corretgé, L., El-biad, M., El-hmidi, H., Fernández, C., Patiño Douceae, A., 2000. Experimental constraints on Hercynian anatexis in the Iberian Massif, Spain. J. Petrol. 41, 1471–1488.
Chen, Y.L., Tang, J.R., Liu, F., Zhang, H.F., Nie, S.L., Jiang, L.T., 2006. Elemental and Sm–Nd isotopic geochemistry of clastic sedimentary rocks in the Garzê-Songpan and Longmen Mountains. Geology in China 33, 109–118 (in Chinese with English abstract).
Chung, S.-L., Chu, M.-F., Zhang, Y., Xie, Y., Lo, C.-H., Lee, T.-Y., Lan, C.-Y., Li, X., Zhang, Q., Wang, Y., 2005. Tibetan tectonic evolution inferred from spatial and temporal variations in post-collisional magmatism. Earth Sci. Rev. 68 (3–4), 173–196.
Chung, S.-L., Lo, C.-H., Lee, T.-Y., Zhang, Y., Xie, Y., Li, X., Wang, K.-L., Wang, P.-L., 1998. Diachronous uplift of the Tibetan Plateau starting 40 Myr ago. Nature 394, 769–773.
Condie, K.C., 1993. Chemical composition and evolution of the upper continental crust: contrasting results from surface samples and shales. Chem. Geol. 104, 1–37.
Condie, K.C., 2005. TTGs and adakites: are they both slab melts? Lithos 80, 33–44.
DeCelles, P.G., Robinson, D.M., Zandt, G., 2002. Implications of shortening in the Himalayan fold-thrust belt for uplift of the Tibetan Plateau. Tectonics 21 (6), 1062. doi:10.1029/2001TC001322.
Defant, M.J., Drummond, M.S., 1990. Derivation of some modern arc magmas by melting of young subducted lithosphere. Nature 347, 662–665.
Defant, M.J., Jackson, T.E., Drummond, M.S., De Boer, J.Z., Bellon, H., Feigenson, M.D., Maury, R.C., Stewart, R.H., 1992. The geochemistry of young volcanism throughout western Panama and southeastern Costa Rica: an overview. J. Geol. Soc. London 149, 569–579.
Defant, M.J., Xu, J.F., Kepezhinskas, P., Wang, Q., Zhang, Q., Xiao, L., 2002. Adakites: some variations on a theme. Acta Petrol. Sin. 18, 129–142.
Deng, W., 1998. Cenozoic Intraplate Volcanic Rocks in the Northern Qinghai–Xizang (Tibetan) Plateau. Geological Publishing House, Beijing. 180 pp.
Deng, W.M., Huang, X., Zhong, D.L., 1998. Alkali-rich porphyries and relationship related to intraplate metamorphosis in the North part of Jinshajiang zone, Dianxi. Science in China, Series D 28, 112–117 (in Chinese).
Ding, L., Kapp, P., Yue, Y., Lai, Q., 2007. Postcollisional calc-alkaline lavas and xenoliths from the southern Qiangtang terrane, central Tibet. Earth Planet. Sci. Lett. 254 (1–2), 28–38.
Ding, L., Kapp, P., Zhong, D., Deng, W., 2003. Cenozoic volcanism in Tibet: evidence for a transition from oceanic to continental subduction. J. Petrol. 44 (10), 1833–1865.
Drummond, M.S., Defant, M.J., Kepezhinskas, P.K., 1996. The petrogenesis of slab derived trondhjemite–tonalite–dacite/adakite magmas. Trans. R. Soc. Edinb. Earth Sci. 87, 205–216.
Dupont-Nivet, G., Krijgsman, W., Langereis, C.G., Abels, H.A., Dai, S., Fang, X., 2007. Tibetan Plateau aridification linked to global cooling at the Eocene–Oligocene transition. Nature 445 (7128), 635–638.
Foley, S.F., Tiepolo, M., Vannucci, R., 2002. Growth of early continental crust controlled by melting of amphibolite in subduction zones. Nature 417, 837–840.
Gao, S., Rudnick, R.L., Yuan, H.L., Liu, X.M., Liu, Y.S., Xu, W.L., Lin, W.L., Ayers, J., Wang, X.C., Wang, Q.H., 2004. Recycling lower continental crust in the North China craton. Nature 432, 892–897.
Guo, Z., Wilson, M., Liu, J., Mao, Q., 2006. Post-collisional, potassic and ultrapotassic magmatism of the northern Tibetan Plateau: constraints on characteristics of the mantle source, geodynamic setting and uplift Mechanisms. J. Petrol. 47 (6), 1177–1220.
Hacker, B.R., Gnos, E., Ratschbacher, L., Grove, M., McWilliams, M., Sobolev, S.V., Wan, J., Zhenhan, W., 2000. Hot and dry deep crustal xenoliths from Tibet. Science 287 (5462), 2463–2466.
Hacker, B.R., Luffi, P., Lutkov, V., Minaev, V., Ratschbacher, L., Plank, T., Ducea, M., Patiño Douceae, A., McWilliams, M., Metcalf, J., 2005. Near-ultrahigh pressure processing of continental crust: Miocene crustal xenoliths from the Pamir. J. Petrol. 46, 1661–1687.
Harris, N., 2006. The elevation history of the Tibetan Plateau and its implications for the Asian monsoon. Palaeogeogr. Palaeoclimatol. Palaeoecol. 241 (1), 4–15.
Harrison, T.M., Copeland, P., Kidd, W.S.F., Yin, A.N., 1992. Raising Tibet. Science 255 (5052), 1663–1670.
Hawkesworth, C.J., Turner, S.P., McDermott, F., Peate, D.W., van Calsteren, P., 1997. U–Th isotopes in arc magmas: implications for element transfer from the subducted crust. Science 276, 551–555.
Hou, Z.Q., Gao, Y.F., Qu, X.M., Rui, Z.Y., Mo, X.X., 2004. Origin of adakitic intrusives generated during mid-Miocene east–west extension in southern Tibet. Earth Planet. Sci. Lett. 220 (1–2), 139–155.
Jackson, S.E., Pearson, N.J., Belousova, E., Griffin, W.L., 2004. The application of laser ablation-inductively coupled plasma-mass spectrometry (LA-ICP-MS) to in situ U–Pb geochronology. Chem. Geol. 211, 47–69.
Jian, P., Liu, D.Y., Sun, X.M., 2003. SHRIMP dating of Carboniferous Jinshajiang ophiolite in western Yunnan and Sichuan: geochronological constraints on the evolution of the Paleo-Tethys oceanic crust. Acta Geologica Sinica 77, 217–277 (in Chinese with English abstract).
Jiang, Y.-H., Jiang, S.-Y., Ling, H.-F., Dai, B.-Z., 2006. Low-degree melting of a metasomatized lithospheric mantle for the origin of Cenozoic Yulong monzogranite-porphyry, east Tibet:

geochemical and Sr–Nd–Pb–Hf isotopic constraints. Earth Planet. Sci. Lett., 241 (3–4), 617–633.
Johnson, M.C., Plank, T., 1999. Dehydration and melting experiments constrain the fate of subducted sediments. Geochem., Geophys., Geosyst. 1 1999GC000014.
Jull, M., Kelemen, P.B., 2001. On the conditions for lower crustal convective instability. J. Geophys. Res. 106, 6423–6446.
Kapp, P., Murphy, M.A., Yin, A., Harrison, T.M., Ding, L., Guo, J., 2003. Mesozoic and Cenozoic tectonic evolution of the Shiquanhe area of western Tibet. Tectonics 22 (4), 1043. doi:10.1029/2002TC001383.
Kapp, P., Yin, A., Harrison, T.M., Ding, L., 2005. Cretaceous–Tertiary shortening, basin development, and volcanism in central Tibet. Geol. Soc. Am. Bull. 117 (7), 865–878.
Kay, R.W., Kay, S.M., 1993. Delamination and delamination magmatism. Tectonophysics 219, 177–189.
Kay, R.W., Kay, S.M., 2002. Andean adakites: three ways to make them. Acta Petrol. Sin. 18, 303–311.
Kay, S.M., Ramos, V.A., Marquez, M., 1993. Evidence in Cerro Pampa volcanic rocks of slab melting prior to ridge trench collision in southern South America. J. Geol. 101, 703–714.
Kelemen, P.B., 1995. Genesis of high Mg andesites and the continental crust. Contrib. Mineral. Petrol. 120, 1–19.
Kelemen, P.B., Yogodzinski, G.M., Scholl, D.W., 2003. Along strike variation in the Aleutian island arc: genesis of high-Mg# andesite and implications for continental crust. In: Eiler, J. (Ed.), Inside the Subduction Factory. Geophysical Monograph, vol. 138. American Geophysical Union, pp. 223–276.
Kind, R., Yuan, X., Saul, J., Nelson, D., Sobolev, S.V., Mechie, J., Zhao, W., Kosarev, G., Ni, J., Achauer, U., Jiang, M., 2002. Seismic images of crust and upper mantle beneath Tibet: evidence for Eurasian plate subduction. Science 298 (5596), 1219–1221.
Kohn, M.J., Parkinson, C.D., 2002. Petrologic case for Eocene slab breakoff during the Indo-Asian collision. Geology 30 (7), 591–594.
Kumar, P., Yuan, X., Kind, R., Ni, J., 2006. Imaging the colliding Indian and Asian lithospheric plates beneath Tibet. J. Geophys. Res. 111 (B6), 1–11. doi:10.1029/2005JB003930 B06308.
Lai, S.C., Liu, C.Y., Yi, H.S., 2003. Geochemistry and petrogenesis of Cenozoic andesite–dacite associations from the Hoh Xil Region, Tibetan Plateau. Int. Geol. Rev. 45 (11), 998–1019.
Li, X.-H., Li, Z.-X., Zhou, H., Liu, Y., Kinny, P.D., 2002a. U–Pb zircon geochronology, geochemistry and Nd isotopic study of Neoproterozoic bimodal volcanic rocks in the Kangdian Rift of South China: implications for the initial rifting of Rodinia. Precambrian Res. 113 (1–2), 135–154.
Li, X.H., Liu, D.Y., Sun, M., Li, W.X., Liang, X.R., Liu, Y., 2004. Precise Sm–Nd and U–Pb isotopic dating of the super-giant Shizhuyuan polymetallic deposit and its host granite, Southeast China. Geol. Mag. 141, 225–231.
Li, Y.P., Lin, Z.H., Zheng, J.B., Yi, S.Q., Teng, Y.H., Wang, X.Y., 2005. Geochemical characteristics and their tectonic implications of early Yanshan granitoid in Shuanghu area of Qiangtang basin of Tibet. Petroleum Geology and Oilfield Development in Daqing 24 (24), 20–24.
Li, Z.X., Li, X.H., Kinny, P.D., Wang, J., Zhang, S., Zhou, H., 2003. Geochronology of neoproterozoic syn-rift magmatism in the Yangtze Craton, South China and correlations with other continents: evidence for a mantle superplume that broke up Rodinia. Precambrian. Res. 122 (1–4), 85–109.
Liang, H.-Y., Campbell, I., Allen, C., Sun, W.-D., Yu, H.-X., Xie, Y.-W., Zhang, Y.-Q., 2007. The age of the potassic alkaline igneous rocks along the Ailao Shan-Red River shear zone: implications for the onset age of left-lateral shearing. J. Geol. 115, 231–242.
Liao, L.G., Cao, S.H., Xiao, Y.B., Ou Yang, K.G., Hu, Z.R., Feng, G.S., 2005. The delineation and significance of the continental margin volcanic magmatic arc zone in the northern part of the Bangong–Nujiang suture zone. Sediment Geol. Tethyan Geology 25, 163–170.
Macpherson, C.G., Dreher, S.T., Thirlwall, M.F., 2006. Adakites without slab melting: high pressure differentiation of island arc magma, Mindanao, the Philippines. Earth Planet. Sci. Lett. 243 (3–4), 581–593.
Martin, H., Smithies, R.H., Rapp, R., Moyen, J.F., Champion, D.C., 2005. An overview of adakite, tonalite–trondhjemite–granodiorite (TTG), and sanukitoid: relationships and some implications for crustal evolution. Lithos 79, 1–24.
McKenna, L.W., Walker, J.D., 1990. Geochemistry of crustally derived leucocratic igneous rocks from the Ulugh Muztagh area, northern Tibet and their implications for the formation of the Tibetan Plateau. J. Geophys. Res. 95, 21483–21502.
Meyer, B., Tapponnier, P., Bourjot, L., Metevier, F., Gaudemer, Y., Peltzer, G., Guo, S., Chen, Z., 1998. Crustal thickening in Gansu–Qinghai, lithospheric mantle subduction, and oblique, strike-slip controlled growth of the Tibet plateau. Geophys. J. Int. 135, 1–47.
Miller, C.F., McDowell, S.M., Mapes, R.W., 2003. Hot and cold granites? Implications of zircon saturation temperatures and preservation of inheritance. Geology 31 (6), 529–532.
Mo, X., Zhao, Z., Deng, J., Flower, M., Yu, X., Luo, Z., Li, Y., Zhou, S., Dong, G., Zhu, D., Wang, L., 2006. Petrology and geochemistry of post-collisional volcanic rocks from the Tibetan Plateau: implications for lithosphere heterogeneity and collision induced asthenospheric mantle flow. In: Dilek, Yildirim, Pavlides, Spyros (Eds.), Postcollisional Tectonics and Magmatism in the Mediterranean Region and Asia. Geological Society of America Special Paper, vol. 409, pp. 507–530.
Molnar, P., England, P., Martinod, J., 1993. Mantle dynamics, uplift of the Tibetan Plateau, and the Indian Monsoon. Rev. Geophys. 31 (4), 357–396.
Molnar, P., Tapponnier, P., 1975. Cenozoic tectonics of Asia: effects of a continental collision. Science 189, 419–426.
Niu, Y., Batiza, R., 1997. Trace element evidence from seamounts for recycled oceanic crust in the eastern equatorial Pacific mantle. Earth Planet. Sci. Lett. 148, 471–484.
Pearce, J.A., Harris, N.B.W., Tindle, A.G., 1984. Trace element discrimination diagrams for the tectonic interpretation of granitic rocks. J. Petrol. 25 (4), 956–983.
Plank, T., 2005. Constraints from thorium/lanthanum on sediment recycling at subduction zones and the evolution of the continents. J. Petrol. 46 (5), 921–944.
Plank, T., Langmuir, C.H., 1993. Tracing trace elements from sediment input to volcanic output at subduction zones. Nature 362, 739–742.
Plank, T., Langmuir, C.H., 1998. The chemical composition of subducting sediment and its consequences for the crust and mantle. Chem. Geol. 145, 325–394.
Prell, W.L., Kutzbach, J.E., 1992. Sensitivity of the Indian Monsoon to forcing parameters and implications for its evolution. Nature 360, 647–652.
Priestley, K., Debayle, E., McKenzie, D., Pilidou, S., 2006. Upper mantle structure of eastern Asia from multimode surface waveform tomography. J. Geophys. Res. 111 (B10), 1–20.
Prouteau, G., Scaillet, B., 2003. Experimental constraints on the origin of the 1991 Pinatubo dacite. J. Petrol. 44 (12), 2203–2241.
Rapp, R.P., Shimizu, N., Norman, M.D., 2003. Growth of early continental crust by partial melting of eclogite. Nature 425, 605–609.
Rapp, R.P., Shimizu, N., Norman, M.D., Applegate, G.S., 1999. Reaction between slab-derived melts and peridotite in the mantle wedge: experimental constraints at 3.8 GPa. Chem. Geol. 160, 335–356.
Raymo, M.E., Ruddiman, W.F., 1992. Tectonic forcing of Late Cenozoic climate. Nature 359, 117–122.
Renne, P.R., Swisher, C.C., Deino, A.L., Karner, D.B., Owens, T.L., DePaolo, D.J., 1998. Intercalibration of standards, absolute ages and uncertainties in $^{40}Ar/^{39}Ar$ dating. Chem. Geol. 145, 117–152.
Roger, F., Calassou, S., 1997. U–Pb geochronology on zircon and isotopic geochemistry (Pb, Sr and Nd) of the basement in the Songpan-Garze fold belt (China). C. R. Acad. Sci., IIA, Earth Planet. Sci. 324, 819–826.
Roger, F., Tapponnier, P., Arnaud, N., Schärer, U., Brunel, M., Xu, Z., Yang, J., 2000. An Eocene magmatic belt across central Tibet: mantle subduction triggered by the Indian collision? Terra Nova 12, 102–108.
Rowley, D.B., Currie, B.S., 2006. Palaeo-altimetry of the Late Eocene to Miocene Lunpola basin, central Tibet. Nature 439 (7077), 677–681.
Ruddiman, W., 1998. Early uplift in Tibet? Nature 394, 723–725.
Schmidt, M.W., Vielzeuf, D., Auzanneau, E., 2004. Melting and dissolution of subducting crust at high pressures: the key role of white mica. Earth Planet. Sci. Lett. 228, 65–84.
Schwab, M., Ratschbacher, L., Siebel, W., McWilliams, M., Minaev, V., Lutkov, V., Chen, F., Stanek, K., Nelson, B., Frisch, W., Wooden, J.L., 2004. Assembly of the Pamirs: age and origin of magmatic belts from the southern Tien Shan to the southern Pamirs and their relation to Tibet. Tectonics 23 (4), TC4002. doi:10.1029/2003TC001583.
She, Z., Ma, C., Mason, R., Li, J., Wang, G., Lei, Y., 2006. Provenance of the Triassic Songpan-Ganzi flysch, west China. Chem. Geol. 231 (1–2), 159–175.
Shi, D., Zhao, W., Brown, L., Nelson, D., Zhao, X., Kind, R., Ni, J., Xiong, J., Mechie, J., Guo, J., Klemperer, S., Hearn, T., 2004. Detection of southward intracontinental subduction of Tibetan lithosphere along the Bangong–Nujiang suture by P-to-S converted waves. Geology 32 (3), 209–212.
Shimoda, G., Tatsumi, Y., Nohda, S., Ishizaka, K., Jahn, B.M., 1998. Setouchi high-Mg andesites revisited; geochemical evidence for melting of subducting sediments. Earth Planet. Sci. Lett. 160, 479–492.
Song, X.-Y., Zhou, M.-F., Cao, Z.-M., Robinson, P.T., 2004. Late Permian rifting of the South China Craton caused by the Emeishan mantle plume? J. Geol. Soc. London 161 (5), 773–781.
Spurlin, M.S., Yin, A., Horton, B.K., Zhou, J., Wang, J., 2005. Structural evolution of the Yushu-Nangqian region and its relationship to syncollisional igneous activity, east-central Tibet. Geol. Soc. Am. Bull. 117 (9), 1293–1317.
Steiger, R.H., Jäger, E., 1977. Subcommission on geochronology: convention on the use of decay constants in geo- and cosmochronology. Earth Planet. Sci. Lett. 36, 359–362.
Stern, C.R., Kilian, R., 1996. Role of the subducted slab, mantle wedge and continental crust in the generation of adakites from the Austral Volcanic Zone. Contrib. Mineral. Petrol. 123, 263–281.
Streck, M.J., Leeman, W.P., Chesley, J., 2007. High-magnesian andesite from Mount Shasta: a product of magma mixing and contamination, not a primitive mantle melt. Geology 35 (4), 351–354.
Sun, S.S., McDonough, W.F., 1989. Chemical and isotopic systematics of oceanic basalts: implications for mantle composition and processes. In: Saunders, A.D., Norry, M.J. (Eds.), Implications for Mantle Composition and Processes, Magmatism in the Ocean Basins. Geological Society Special Publication, pp. 313–345.
Tapponnier, P., Zhiqin, X., Roger, F., Meyer, B., Arnaud, N., Wittlinger, G., Jingsui, Y., 2001. Oblique stepwise rise and growth of the Tibet plateau. Science 294 (5547), 1671–1677.
Tatsumi, Y., 2001. Geochemical modeling of partial melting of subducting sediments and subsequent melt–mantle interaction: generation of high-Mg andesites in the Setouchi volcanic belt, southwest Japan. Geology 29, 323–326.
Tatsumi, Y., Hanyu, T., 2003. Geochemical modeling of dehydration and partial melting of subducting lithosphere: toward a comprehensive understanding of high-Mg andesite formation in the Setouchi volcanic belt, SW Japan. Geochem., Geophys., Geosyst. 4, 1081. doi:10.1029/2003GC000530.
Turner, S., Arnaud, N., Liu, J., Rogers, N., Hawkesworth, C., Harris, N., Kelley, S., Van Calsteren, P., Deng, W., 1996. Post-collision, shoshonitic volcanism on the Tibetan Plateau: implications for convective thinning of the lithosphere and the source of ocean island basalts. J. Petrol. 37 (1), 45–71.
Vasconcelos, P.M., 1999. K–Ar and $^{40}Ar/^{39}Ar$ geochronology of weathering processes. Annu. Rev. Earth Planet. Sci. 27, 183–229.
Vergne, J., Wittlinger, G., Hui, Q., Tapponnier, P., Poupinet, G., Mei, J., Herquel, G., Paul, A., 2002. Seismic evidence for stepwise thickening of the crust across the NE Tibetan Plateau. Earth Planet. Sci. Lett. 203 (1), 25–33.
Wang, C., Liu, Z., Yi, H., Liu, S., Zhao, X., 2002. Tertiary crustal shortening and peneplanation in the Hoh Xil region: implications for the tectonic history of the northern Tibetan Plateau. J. Asian Earth Sci. 20 (3), 211–223.

Wang, J.-H., Yin, A., Harrison, T.M., Grove, M., Zhang, Y.-Q., Xie, G.-H., 2001. A tectonic model for Cenozoic igneous activities in the eastern Indo-Asian collision zone. Earth Planet. Sci. Lett. 188 (1–2), 123–133.

Wang, Q., McDermott, F., Xu, J.F., Bellon, H., Zhu, Y.T., 2005. Cenozoic K-rich adakitic volcanic rocks in the Hohxil area, northern Tibet: lower-crustal melting in an intracontinental setting. Geology 33, 465–468.

Wang, Q., Wyman, D.A., Zhao, Z.H., Xu, J.F., Bai, Z.H., Xiong, X.L., Dai, T.M., Li, C.F., Chu, Z.Y., 2007a. Petrogenesis of carboniferous adakites and Nb-enriched arc basalts in the Alataw area, northern Tianshan Range (western China): implication for phanerozoic crustal growth of Central Asia Orogenic Belt. Chem. Geol. 236, 42–64.

Wang, Q., Wyman, D.A., Xu, J., Jian, P., Zhao, Z., Li, C., Xu, W., Ma, J., He, B., 2007b. Early Cretaceous adakitic granites in the Northern Dabie Complex, central China: implications for partial melting and delamination of thickened lower crust. Geochim. Cosmochim. Acta 71 (10), 2609–2636.

Wang, Q., Xu, J.F., Jian, P., Bao, Z.W., Zhao, Z.H., Li, C.F., Xiong, X.L., Ma, J.L., 2006. Petrogenesis of adakitic porphyries in an extensional tectonic setting, Dexing, South China: implications for the genesis of porphyry copper mineralization. J. Petrol. 47, 119–144.

Wang, Q., Wyman, A., Xu, J.F., Wan, Y.S., Li, C.F., Zi, F., Jiang, Z.Q., Qiu, H.N., Chu, Z.Y., Zhao, Z.H., Dong, Y.H., 2008. Triassic Nb-enriched basalts, magnesian andesites, and adakites of the Qiangtang terrane (Central Tibet): evidence for metasomatism by slab-derived melts in the mantle wedge. Contrib. Mineral. Petrol. 155, 473–490.

Wang, Y.B., 2005. The structure and evolution of Middle Permian ancient seamounts in the Bayakala and nearby areas. Science in China (Series D) 35, 1140–1149 (In Chinese).

Wei, G.J., Liang, X.R., Li, X.H., Liu, Y., 2002. Precise measurement of Sr isotopic composition of liquid and solid base suing (LP) MC-ICPMS. Geochimica 31, 35–42 (in Chinese with English abstract).

Williams, H.M., Turner, S.P., Pearce, J.A., Kelley, S.P., Harris, N.B.W., 2004. Nature of the source regions for post-collisional, potassic magmatism in southern and northern Tibet from geochemical variations and inverse trace element modelling. J. Petrol. 45 (3), 555–607.

Wittlinger, G., Vergne, J., Tapponnier, P., Farra, V., Poupinet, G., Jiang, M., Su, H., Herquel, G., Paul, A., 2004. Teleseismic imaging of subducting lithosphere and Moho offsets beneath western Tibet. Earth Planet. Sci. Lett. 221 (1–4), 117–130.

Xiao, L., Clemens, J.D., 2007. Origin of potassic (C-type) adakite magmas: experimental and field constraints. Lithos 95 (3–4), 399–414.

Xiao, L., Xu, J.F., 2005. Petrogenesis and tectonic setting of Dashibao Group basalts from Songpan-Ganze block, northwestern Sichuan province, China. Acta Petrol. Sin. 21 (6), 1539–1545.

Xiong, X.L., Adam, J., Green, T.H., 2005. Rutile stability and rutile/melt HFSE partitioning during partial melting of hydrous basalt: implications for TTG genesis. Chem. Geol. 218 (3–4), 339–359.

Xu, J.F., Shinjo, R., Defant, M.J., Wang, Q., Rapp, R.P., 2002. Origin of Mesozoic adakitic intrusive rocks in the Ningzhen area of east China: partial melting of delaminated lower continental crust? Geology 30 (12), 1111–1114.

Xu, Y.G., Chung, S.L., Jahn, B.M., Wu, G.Y., 2001. Petrological and geochemical constraints on the petrogenesis of the Permo-Triassic Emeishan Flood basalts in southwestern China. Lithos 58, 145–168.

Yin, A., Harrison, T.M., 2000. Geologic evolution of the Himalayan—Tibetan orogen. Ann. Rev. Earth Planet. Sci. 28, 211–280.

Zhang, H.F., Sun, M., Zhou, X.H., Fan, W.M., Zhai, M.G., Yin, J.F., 2002. Mesozoic lithosphere destruction beneath the North China Craton: evidence from major-, trace- element and Sr–Nd–Pb isotope studies of Fangcheng basalts. Contrib. Mineral. Petrol. 144, 241–253.

Zhang, H.F., Zhang, L., Harris, N., Jin, L.L., Yuan, H.L., 2006. U–Pb zircon ages, geochemical and isotopic compositions of granitoids in Songpan-Garze fold belt, eastern Tibetan Plateau: constraints on petrogenesis and tectonic evolution of the basement. Contrib. Mineral. Petrol. 152, 75–88.

Zhou, J., Xu, F., Wang, T., Cao, A., Yin, C., 2006a. Cenozoic deformation history of the Qaidam Basin, NW China: results from cross-section restoration and implications for Qinghai–Tibet Plateau tectonics. Earth Planet. Sci. Lett. 243 (1–2), 195–210.

Zhou, M.F., Yan, D.P., Wang, C.L., Liang, Q., Kennedy, A., 2006b. Subduction-related origin of the 750 Ma Xuelongbao adakitic complex (Sichuan Province, China): implications for the tectonic setting of the giant Neoproterozoic magmatic event in South China. Earth Planet. Sci. Lett. 248 (1–2), 286–300.